Gondwana Research 27 (2015) 1430–1445

Contents lists available at ScienceDirect

Gondwana Research

journal homepage: www.elsevier.com/locate/gr

Thermal and petrophysical characterization of the lithospheric mantle along the northeastern Iberia geo-transect

A. Carballo *, M. Fernandez, M. Torne, I. Jiménez-Munt, A. Villaseñor

Group of Dynamics of the Lithosphere, Institute of Earth Sciences Jaume Almera, ICTJA — CSIC, Lluis Sole i Sabaris s/n, 08028 Barcelona, Spain

ARTICLE INFO

Article history:
Received 25 September 2013
Received in revised form 18 December 2013
Accepted 23 December 2013
Available online 21 January 2014

Handling Editor: A.R.A. Aitken

Keywords:
Upper mantle composition
Iberia
Western Mediterranean
Potential fields
Thermal modeling

ABSTRACT

We present a new model on the present-day lithospheric structure along a 1100 km transect crossing the NE-Iberian Peninsula, the Western Mediterranean basin and the Algeria margin and ends at the Tell–Atlas Mountains. The modeling is based on an integrated geophysical-petrological methodology combining elevation, gravity, geoid, surface heat flow, seismic and geochemical data. Unlike previous models proposed for the region where the density of the lithospheric mantle is only temperature-dependent, the applied methodology allows inferring seismic velocities and density in the mantle down to 410 km depth from its chemical composition through self-consistent thermodynamic calculations. We have considered five lithospheric mantle compositions including predominantly average Phanerozoic and lherzolitic Proterozoic in the continental mainland, and more fertile PUM (primitive upper mantle) compositions in the Western Mediterranean basin. Mantle petrology affects the resulting density distribution and LAB (lithosphere–asthenosphere boundary) geometry and allows a direct comparison with tomography models and seismic data. Measured low Pn velocities in the Western Mediterranean basin can be explained by either serpentinization and/or seismic anisotropy and only partly by transient thermal effects. The obtained lithospheric structure is compatible with P- and S-wave tomography models.

1. Introduction

The present-day lithospheric structure of Iberia and the western Mediterranean region is the result of a complex and puzzling moving of the Iberian microplate that started in early Cretaceous times with the northward propagation of the Atlantic Ocean, and the Alpine collision of the northward moving African plate with stable Europe. The relative and complex motions of Iberia, Africa and Europe have given rise to numerous tectonic reconstructions of the Alpine–Mediterranean region (e.g., Rosenbaum and Lister, 2002; Stampfli and Borel, 2002; Handy et al., 2010; Schettino and Turco, 2010; Vissers and Meijer, 2012). According to these reconstructions, the northern convergence of Africa against Europe was accommodated by the development of two subduction zones affecting the northern and southeastern Iberian margins. The north Iberian margin evolved from the tectonic inversion of a Mesozoic rift system (Vergés and García-Senz, 2001) and resulted in the formation of the Pyrenean fold-and-thrust belt and its foreland basins, the Aquitanian and the Ebro basins (Fig. 1), which are a classic example of a continent–continent collision zone (e.g., Muñoz, 1992; Vergés et al., 2002; Sibuet et al., 2004; Vissers and Meijer, 2012) accompanied by an incipient subduction of Iberia underneath the Eurasian plate. The southeast Iberian margin evolved in a more complex subduction pattern of the Mesozoic Ligurian-Tethys ocean with either a NW-dipping subduction affecting part or the whole present-day Iberian Mediterranean margin (e.g., Gueguen et al., 1998; Faccenna et al., 2004; Rosenbaum and Lister, 2004; Spakman and Wortel, 2004), or with lateral changes in the subduction polarity dipping towards the NW in the proto-Algerian segment and towards the SE in the proto-Alboran segment (Vergés and Fernàndez, 2012). Subduction took place first along the Iberia–Eurasia plate boundary (Late Cretaceous to mid-Eocene) and later on along the Iberia–Africa plate boundary (mid-Eocene to Late Oligocene). While in north Iberia convergence was the predominant deformation mechanism, in the western Mediterranean area (Valencia Trough and Algerian Basin) coeval convergence and divergence are observed. A back-arc origin of these basins related to the combination of the northern motion of the African plate and the southeastward retreat of the Tethyan subducting slab was proposed to explain coeval extension and tectonic shortening in this region (e.g., Doglioni et al., 1997; Gueguen et al., 1998; Vergés and Sàbat, 1999; Faccenna et al., 2004). The north African margin in Algeria, presently under compression (Stich et al., 2003; Deverchere et al., 2005; Domzig et al., 2006), is formed by the piling up of metamorphic slices corresponding to the Kabylies and thrusting sheets of Mesozoic and Tertiary sediments in the Tell–Atlas region (e.g., Frizon de Lamotte et al., 2000; Mauffret, 2007).

Thereby, the present-day crustal and lithospheric mantle structure in SE-Iberia and the western Mediterranean is the result of compressional tectonics with collision/subduction in the former Eurasia–Iberia (Pyrenees) and in the Iberia–Africa (Tell–Atlas) plate boundaries, and back-arc extensional tectonics in the Neogene western Mediterranean. This complex tectonic evolution affected Paleozoic, Mesozoic and Tertiary domains with late-Hercynian plutonism in the Pyrenees

* Corresponding author.
E-mail addresses: acarballo@ictja.csic.es, albertocarballo.g@gmail.com (A. Carballo).

1342-937X/$ – see front matter © 2014 International Association for Gondwana Research. Published by Elsevier B.V. All rights reserved.
http://dx.doi.org/10.1016/j.gr.2013.12.012

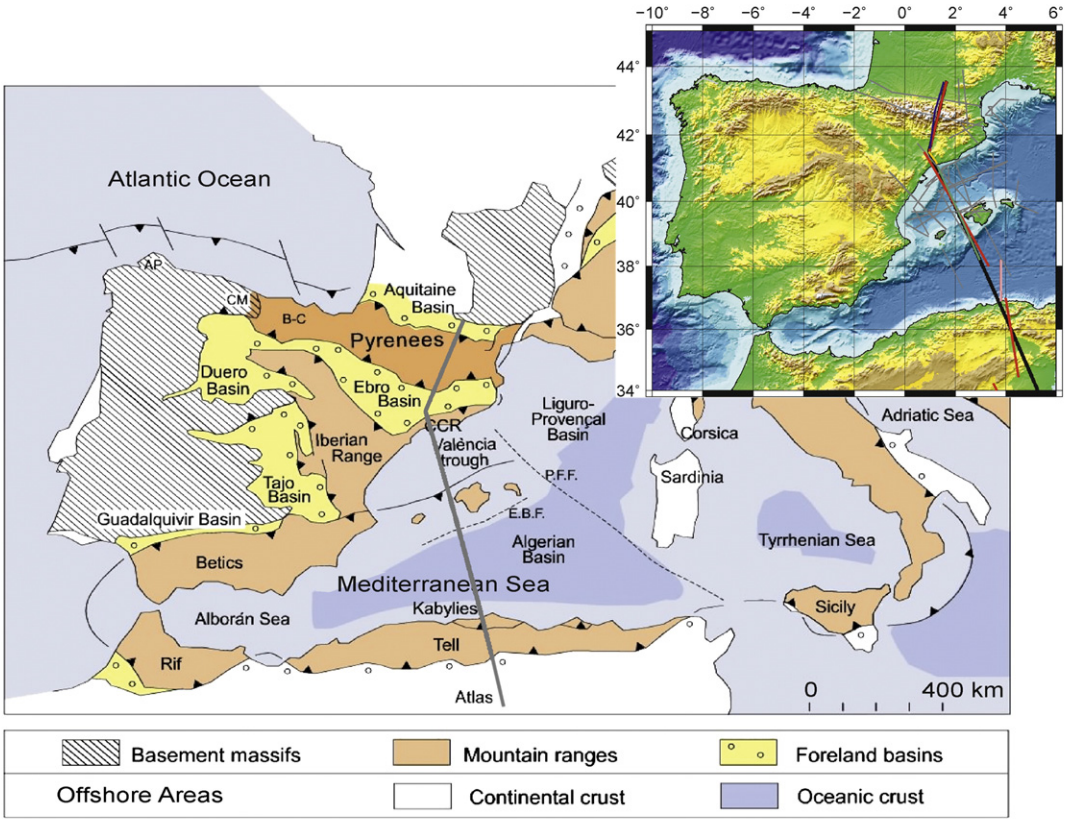

Fig. 1. Geological map of the study area showing the principal geological domains of Iberia, Western Mediterranean and North Africa. Thick gray line locates the modeled transect. Upper right inset shows the main topography and bathymetry features of the study area in which we have located from N to S: Black line-model transect; Deep blue—ECORS Pyrenees; Yellow—ESCI Catalanides; Green line—ESCI València; Pink line: ALE-4 and dark gray-other seismic experiments (Diaz et al., 201X). (see text for details).
Modified from Vergés and Sàbat (1999).

(Michard-Vitrac et al., 1980; Fourcade and Allègre, 1981) and Neogene volcanism along the Iberian–Mediterranean margin (Martí et al., 1992; Wilson and Bianchini, 1999; Lustrino et al., 2011) and generation of oceanic crust in the Algerian Basin (Sàbat et al., 1997; Vidal et al., 1998; Booth-Rea et al., 2007). The succession of these tectonothermal events has probably modified the chemical composition of the lithospheric mantle as observed at global scale (e.g., Poudjom Djomani et al., 2001; Griffin et al., 2009) with relevant implications in the geometry of the crust–mantle and lithosphere–asthenosphere boundaries. Up to date however, a quantified thermal and petrophysical characterization of the lithospheric mantle in NE-Iberia and western Mediterranean consistent with the tectonothermal evolution of the region has not been attempted.

Unraveling the crust and lithosphere structure of the Alpine-Mediterranean region has been the subject in the last decades of numerous geological and geophysical studies that were summarized in eight regional geo-transects in the TRANSMED Atlas (Cavazza et al., 2004). Among these, the TRANSMED-II geo-transect (Roca et al., 2004) begins with a N–S trend crossing the southern part of the Aquitanian basin, the Pyrenees and the northern part of the Eastern Ebro Basin. Then it continues with a NNW–SSE direction through the southern part of the Eastern Ebro Basin, the Catalan Coastal Ranges, the Valencia Trough Basin, the Balearic Promontory, the Algeria Basin, the North African margin, the Kabylies, and ending at the Tell–Atlas mountain range (Fig. 1). Whereas the crustal structure is well defined from the numerous seismic surveys and combined seismic and gravity models (e.g., ECORS Pyrenees Team, 1988; Gallart et al., 1994; Vidal et al., 1998; Roca et al., 2004 and references therein), the depth to lithosphere–asthenosphere boundary (LAB) remains more uncertain due to the lack of direct observables and its more elusive definition (Eaton et al., 2009; Fischer et al., 2010). Existing integrated models based on the combination of elevation, gravity, geoid, heat flow and crustal seismic data show LAB depth varying from more than 130 km beneath the Pyrenees to less than 70 km beneath the western Mediterranean basins (Zeyen and Fernandez, 1994; Ayala et al., 1996, 2003; Roca et al., 2004). All these models however are based on a pure thermal approach in which the density of the lithospheric mantle is only temperature dependent and related to the density of the asthenosphere that, in turn, is considered constant everywhere (Lachenbruch and Morgan, 1990). A major caveat of this approach is the lack of full consistency with the petrophysical properties of the mantle (density and elastic parameters) and therefore, the obtained results cannot be properly compared with seismic data or tomography models. In addition, the contribution of chemical composition and phase transitions on the density and buoyancy of the lithospheric mantle and therefore, on the resulting lithospheric structure (Afonso et al., 2008; Fullea et al., 2010) are not accounted for.

A major observation in the Valencia Trough and the Algerian Basin is the low Pn-velocity values obtained in seismic experiments, which range from 7.7 to 7.95 km/s (Torne et al., 1992; Danobeitia et al., 1992; Vidal et al., 1998; Grevemeyer, pers. comm.) and the noticeable seismic anisotropy, which amounts up to 4.5% and shows almost orthogonal fast polarization directions (FPD) in both basins (Díaz et al., 2013). Low P-wave upper mantle velocities in extensional regions have been traditionally interpreted in terms of thermal relaxation, compositional crust–mantle transition, and underplating (e.g., Morgan and Ramberg, 1987; Collier et al., 1994; Thybo and Artemieva, in press) but effects of anisotropy, thermal disequilibrium and presence of water in the uppermost mantle have not been fully considered in these basins.

In this context, the aim of this work is three-fold: a) to obtain a more reliable structure of the lithosphere along the model transect incorporating, for the first time, petrophysical and geochemical constraints to characterize the lithospheric mantle; b) to analyze, along the model transect, the influence of lateral changes in the composition of the lithosphere mantle on the resulting LAB geometry and how it compares with previous 2D modeling results and c) to decipher the still unresolved origin of the observed low uppermost mantle Pn velocities beneath the Valencia and Algerian basins and their margins.

To this end, a 2D modeling along a 1100 km long profile coinciding with the TRANSMED-II geo-transect has been performed using the LitMod finite-element code developed by Afonso et al. (2008). This new integrated geophysical–petrological methodology allows studying the thermal, compositional, density and seismological structure of the upper mantle down to 410 km depth. The method uses a self-consistent thermodynamic–geophysical framework, in which all relevant properties are functions of temperature, pressure, and mineral composition allowing for the incorporation of lateral compositional variations in the lithospheric mantle and for the direct comparison with seismic data and tomography models.

2. Geological setting

For the sake of simplicity and to facilitate comprehension of the complex tectonic scenario of the study region we describe the geological setting using the chronology of deformation events for each structural domain. This contribution does not intend to present a thorough description of the geology of the study region, thus for a more detailed information the reader is referred to the works of Ziegler and Roure (1996), Torné et al. (1996), Vergés and Sàbat (1999), Cavazza et al. (2004) and Roca et al. (2004), among others.

2.1. The Pyrenean domain (Late Cretaceous–middle Oligocene)

To the North, the Pyrenean fold-thrust belt is a classic example of continent–continent collision that initiated by late Senonian and ceased at middle Oligocene. With a length of about 450 km, the belt runs in an E–W direction, from the Gulf of Lyon to the E to the Gulf of Biscay to the W (see Fig. 1 for location). The orogen is an asymmetrical and bivergent V-shaped continental wedge, the northern wedge being formed by a series of northward directed thrusts on top of the European plate, while the southern wedge, on top of the Iberian plate, is wider and shows greater displacement and shortening. From North to South the Pyrenees orogen comprises the Aquitaine foreland basin; the North Pyrenean thrust system; the axial zone, mainly composed by metamorphic and igneous rocks; the South Pyrenean thrust system and the Ebro foreland basin (e.g., Muñoz et al., 1986; Muñoz, 1992; Verges et al., 1995; Muñoz, 2002).

At crustal and lithospheric levels the collision caused a thickening of the crust from about 32 km beneath the Ebro basin to almost 60 km under the axial zone of the Pyrenees (ECORS Pyrenees Team, 1988; Torné et al., 1989) while the LAB deepens from about to 90–110 km to 140–160 km depending on authors (e.g., Zeyen and Fernandez, 1994; Pous et al., 1995; Roca et al., 2004; Gunnell et al., 2008; Campanyà et al., 2012).

Coinciding with the cessation of the main compressive stage along the Pyrenees, which also resulted in the formation of the Catalan Coastal Ranges, deformation migrated to the south and south east into the Valencia Trough and Algerian basins domains (Vergés and Sàbat, 1999). Unlike the Pyrenees, the Catalan Coastal Ranges (see Fig. 1 for location) do not show significant thickening either of the crust or of the mantle lithosphere.

2.2. The Tethyan subduction domain (Late Oligocene–Late Miocene)

The structures related to the Tethyan subduction were mainly developed between the Late Oligocene and Late Miocene (Roca et al., 2004). In the Mediterranean segment of the modeled transect, the crustal and lithosphere geometry is mainly the result of the south-eastward retreat of the Tethys–Maghrebides subduction zone (Doglioni et al., 1997; Carminati et al., 1998; Vergés and Sàbat, 1999). The south-eastward retreat of the slab resulted in a widespread back-arc extension which thinned the southeastern margin of the Iberian plate and caused the opening of the Valencia and Algerian basins.

In the Valencia Trough Basin extension lasted from Late Oligocene to Langhian period, whereas the opening of the Algerian Basin began later (latest Early Miocene–Middle Miocene) and ended during the Tortonian when remnants of the southern Iberia continental margin (the Kabylies) accreted with the African plate. The accretion of the Kabylies led to the development of the Tell thrust system in the northern African domain (Cavazza et al., 2004; Roca et al., 2004).

Back-arc extension resulted in thinning of the crust and lithosphere mantle. In the Valencia Trough Basin the crust thins from 20 to 22 km near the Iberia coastline to 14 km at its central parts (e.g., Pascal et al., 1992; Torne et al., 1992; Gallart et al., 1994; Vidal et al., 1998), while the LAB shallows to as much as 65 to 60 km, depending on the authors (e.g., Zeyen and Fernandez, 1994; Ayala et al., 1996; Roca et al., 2004). A slight thickening of the crust and lithosphere is observed in its southeast margin, along the Balearic Promontory, where the base of the crust and LAB achieves values of about 20 and 90 km, respectively. This thickening is partly explained by the fact that the area was affected by the orogenic activity recorded along the south-eastern passive margin of Iberia from Late Oligocene to Middle Miocene which gave rise to the observed WNW–ENE verging folds and thrust that involve the Mesozic cover and Paleogene to Middle Miocene sediments (e.g., Sàbat et al., 1988; Roca et al., 1999).

The geometry of the crust and lithosphere mantle is not so well constrained along the Algerian basin owing to scarcity of geophysical experiments. In the northwest part of the Algerian basin the available seismic refraction profile of Hinz (1972) shows that the crust is partly oceanic with a thickness of about 5 km. This value is consistent with that observed in the ESCI—Valencia seismic reflection profile (Sàbat et al., 1997; Vidal et al., 1998). Roca et al. (2004) show that the LAB attains depths of about 50 km in the central parts of the basin, abruptly deepening near the African coastline to values of 175–185 km.

From late Miocene, the protracted slow convergence between the African and Eurasian plates (~6 mm/year; Argus et al., 1989; DeMets et al., 1994) has caused intraplate compressive stresses in the whole area, which have resulted in compressive reactivation of previous faults. Active faulting combining ENE–WSW reverse faults and NW–SE right lateral strike-slip faults is particularly important in the Algerian margin as shown by numerous destructive earthquakes (El Asnam, 1980, Ms = 7.3; Boumerdès, 2003, Ms = 6.7). The observed compressive deformation could indicate the development of a new African-Eurasian boundary along the Algerian margin, where the thin Algerian oceanic lithosphere is in contact with the thicker African continental lithosphere (e.g., Deverchere et al., 2005; Domzig et al., 2006).

3. Method and geophysical observables

3.1. Method

The methodology used in this work is based on the *LitMod-2D* code (Afonso et al., 2008), which combines geophysical and petrological data to study the crust and upper mantle structure from a thermal, compositional, seismological and density point of view. The code allows calculating the 2D distribution of temperature, density and mantle seismic velocities down to 410 km depth and the surface heat flow (SHF), elevation, and gravity and geoid anomalies. A comparison of model outputs against observed data is used to obtain a self-consistent lithospheric/sublithospheric model that simultaneously fits all geophysical and petrological observables, and consequently reduces the uncertainties associated with previous thermal approaches. In *LitMod* the mantle is defined according to its chemical composition within the CFMAS system (CaO–FeO–MgO–Al_2O_3–SiO_2) where minor oxides as Cr_2O_3 and Na_2O and water can also be incorporated. Stable mineral assemblages are determined through self-consistent thermodynamic calculations and thus physical properties of each mineral and of the bulk mantle (density, thermal expansion coefficient, elastic parameters, and thermal conductivity) depend not only on temperature as in previous methodology, but also on pressure, composition, and phase changes. Once the bulk physical properties are determined for each mantle composition, gravity, geoid, elevation, surface heat-flow and P- and S-seismic velocities are computed and compared with observations.

The thermal equation is solved by finite elements method in steady-state with the following boundary conditions: 0 °C at the surface; 1330 °C at the LAB; and no heat flow across the lateral boundaries of the model. Beneath the LAB the algorithm considers a thermal buffer layer of about 40 km thick and 1400 °C at its base to avoid unrealistic discontinuities between a conductive thermal gradient within the lithospheric mantle and an adiabatic thermal gradient within the asthenosphere. The temperature at the base of the model (410 km) is set to 1520 °C. The temperature gradient below the thermal buffer layer is restricted to $0.35 < dT/dz < 0.50$ °C/km, otherwise the temperature at 410 km depth is modified accordingly (see Afonso et al., 2008 for further details).

The model follows a forward scheme in which the crustal and lithospheric mantle geometry, crustal rock properties, LAB geometry and chemical composition of lithospheric mantle bodies are modified within the experimental uncertainties in a trial and error procedure until the best fitting model is obtained.

3.2. Regional geophysical data

Regional geophysical data sets (elevation, gravity, SHF, and geoid height; Fig. 2) were collected from different data sources. Elevation data come from ETOPO2v2 Global Data Base (http://www.ngdc.noaa.gov/mgg/fliers/01mgg04.html) (Fig. 2a). Along the transect maximum average elevation values of about 2000 m are attained in the Pyreness, while the minimum is reached in the Algerian Basin where the ocean floor deepens to as much as −2900 m. Onshore Bouguer anomalies (Fig. 2b) were obtained from a recent compilation of gravity data in the Iberian Peninsula (Ayala, 2013). Free-air gravity anomalies offshore and onshore North Africa were obtained from the global satellite

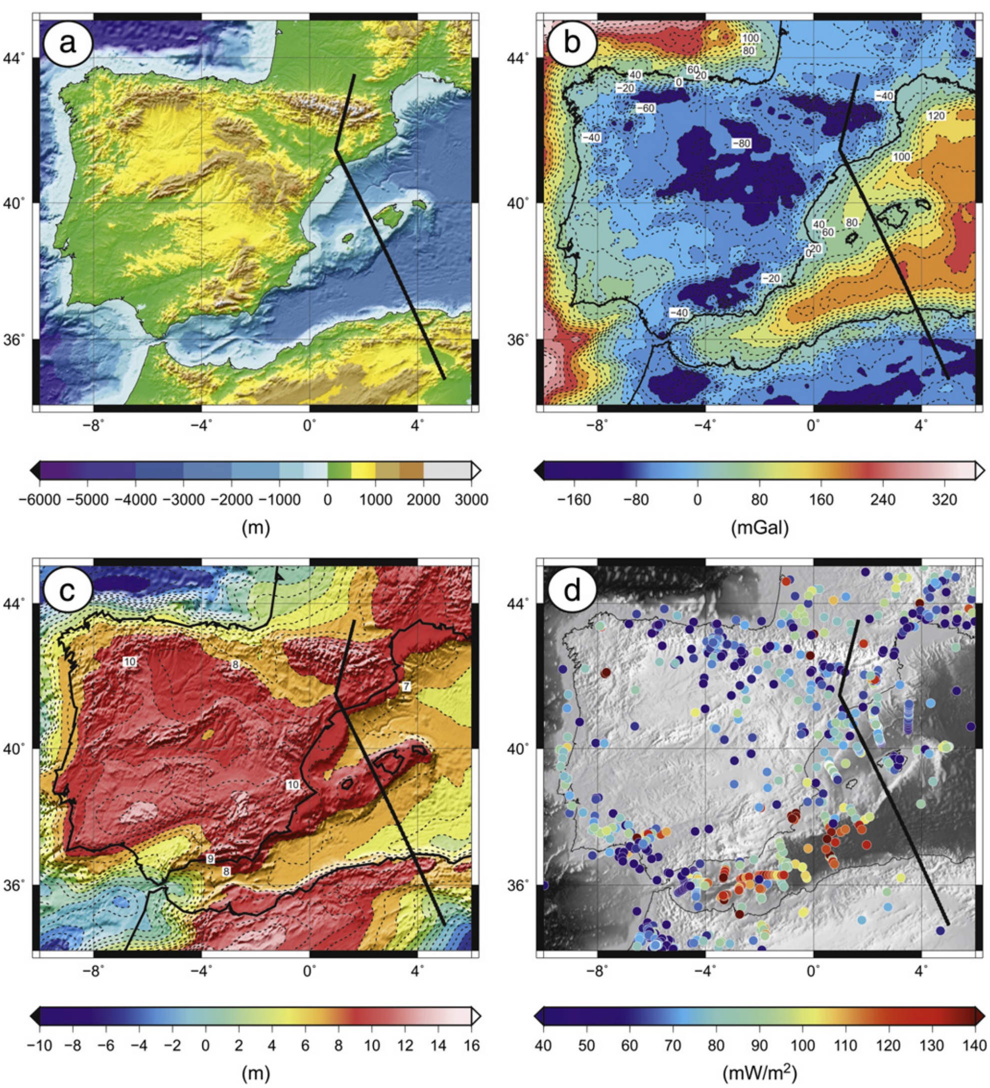

Fig. 2. Geophysical data. a) Elevation map from ETOPO2 Global Data Base (V9.1) (http://www.ngdc.noaa.gov/mgg/fliers/01mgg04.html). b) Bouguer anomaly. Onshore, in the Iberian Peninsula, the Bouguer anomaly comes from Ayala (2013). Offshore and Africa Bouguer anomaly has been calculated from the free air anomaly by Sandwell and Smith (1997) using Fullea et al. (2008). Contour interval is 20 mGal. c) Geoid anomaly map from EGM2008 Global Model (Pavlis et al., 2008). Long wavelengths (>5000 km) have been removed by subtracting spherical harmonics up to degree and order 8 from the total geoid. Contour interval is 1 m. d) Surface heat flow measurements from Fernandez et al. (1998), Marzán Blas (2000) and International Heat Flow Commission global data set for Algeria (http://www.heatflow.und.edu/index2.html). Colors of solid circles indicate heat flow values.

altimetry data model V16.1 (Sandwell and Smith, 1997, updated 2007). Bouguer anomalies (Fig. 2b) were computed from the free-air grid with the software FA2BOUG (Fullea et al., 2008). Minimum Bouguer values of −120 mGal are achieved below the Pyrenees and the Kabylies–Tell–Atlas mountains (−100 mGal), while maximum values are recorded below the Valencia Trough and Algerian basins, 100 and 200 mGal, respectively. Geoid height data were taken from EGM2008 (Pavlis et al., 2008) and filtered up to degree and order 8, to retain only the lithospheric signature. The values for the region vary from 12 m in the Pyrenees, to about 7 and 5 m in the Valencia Trough and Algerian basins, respectively, increasing by 4–5 m in the Kabylies and decreasing steadily to 0 m in the south-end of the transect (Fig. 2c).

SHF data were obtained from Fernandez et al. (1998) in NE-Iberia and its margin, which also incorporates the sea-floor heat flow measurements in the Valencia Trough Basin from Foucher et al. (1992). In the Algerian Basin data were taken from Marzán Blas (2000) whereas in North Africa were taken from Rimi et al. (2005) in Morocco and from the International Heat Flow Commission global data set for Algeria (http://www.heatflow.und.edu/index2.html). Fig. 2d shows the location and values of available measurements. As observed the data exhibit a wide scatter around a mean value of 65 mW m^{-2} onshore and 70–80 mW m^{-2} in the Valencia Trough and the Balearic Promontory, with a very poor coverage in some segments of the model transect, particularly along the Algerian Basin and onshore Algeria. Nevertheless, seafloor heat flow measurements carried out in the western Algeria Basin show values ranging from 90 to 120 mW m^{-2} (Marzán Blas, 2000).

To account for lateral variations perpendicular to the strike of the profile, elevation, gravity, geoid and heat flow data have been projected onto the profile within a strip of 25 km half-width and the resulting standard deviation computed and displayed in Fig. 3 as error bars.

3.3. Crustal and lithosphere mantle geometry from previous studies

The crustal geometry is well known along the model transect from the numerous deep seismic reflection and wide-angle/refraction profiles collected during the last decades (Figs. 1 and 3). The compilation of available crustal structure is summarized in the TRANSMED II transect (Roca et al., 2004). Original seismic data come from ECORS—Central Pyrenees (ECORS Pyrenees Team, 1988), ESCI—Catalánides (Gallart et al., 1994), ESCI—Valencia (Vidal et al., 1998), Hinz (1972) and ALE-4 (an industry profile) (see Fig. 1 for location of profiles). The Moho depth varies from 32 to 35 km beneath the Aquitanian Basin to more than 50 km in the Pyrenees and 36–32 km in the Ebro Basin and Catalan Coastal Ranges. Towards the Valencia Trough, the Moho rises up to 16–18 km deepening to 22–25 km in the Balearic Promontory whereas beneath the Algerian Basin the Moho lies at 10–12 km depth. In the Algerian margin, the Moho depth increases to values of about 30 km close to the shoreline and according to Roca et al. (2004) it deepens down to 40 km depth beneath the Tell–Atlas mountains.

The LAB beneath the model transect and surrounding areas has been the subject of several studies, mainly 2D modeling, integrating different geophysical data sets (e.g., Fernandez et al., 1990; Zeyen and Fernandez, 1994; Ayala et al., 1996, 2003; Roca et al., 2004). As mentioned, most of these models do not consider pressure and compositional changes in the mantle. As pointed out by Afonso et al. (2008) the neglect of compressibility, phase changes and compositional heterogeneities could result in uncertainties in the density contrast at Moho and LAB levels and in turn in the resulting LAB depth. The assumed temperature-dependent mantle density also shows inconsistencies with tomography, xenolith and thermodynamic data. Nevertheless, as a first approach we have used the available information as a first input in our forward modeling. For instance, the works of Fernandez et al. (1990); Zeyen and Fernandez (1994) and Ayala et al. (1996, 2003) have reported lithospheric thickening from 110 to 120 km beneath the foreland basins to as much as 150 km below the axial zone of the Pyrenees. A thickness decrease is observed towards the central region of the Valencia Trough where values of 65–60 km are reported. To the SE, along the Balearic Promontory the thickness of the lithosphere slightly increases (88–92 km), thinning towards the Algerian Basin where the LAB raises to 55 km. Towards the Algerian margin and North-Africa, Roca et al. (2004) imaged a sharp lithospheric thickening with a LAB depth exceeding 160 km.

4. Results

Fig. 4 shows the best fitting model using the parameters summarized in Tables 1 and 2. Density and thermal conductivity values for crustal bodies have been taken from previous studies (e.g., Fernandez et al., 1990; Torne et al., 1992, 1996; Zeyen and Fernandez, 1994). Radiogenic heat production has been taken from a global compilation carried out by Vilà et al. (2010). In the mantle, density has been calculated from its chemical composition whereas thermal conductivity is calculated according to Hofmeister (1999). Mineral assemblages in the lithospheric mantle have been computed using the NCFMAS approach (see Table 2). Our results show that along the model profile we can distinguish five lithospheric mantle types which agree with the geodynamic domains described above. In NE Iberia mainland a Proterozoic (Proton-lherzolite average, Pr_6) as proposed by Griffin et al. (2009) fits the observable geophysical data and is also in agreement with xenolith data collected by Le Roux et al. (2007). In the Valencia Trough and the Balearic Promontory the

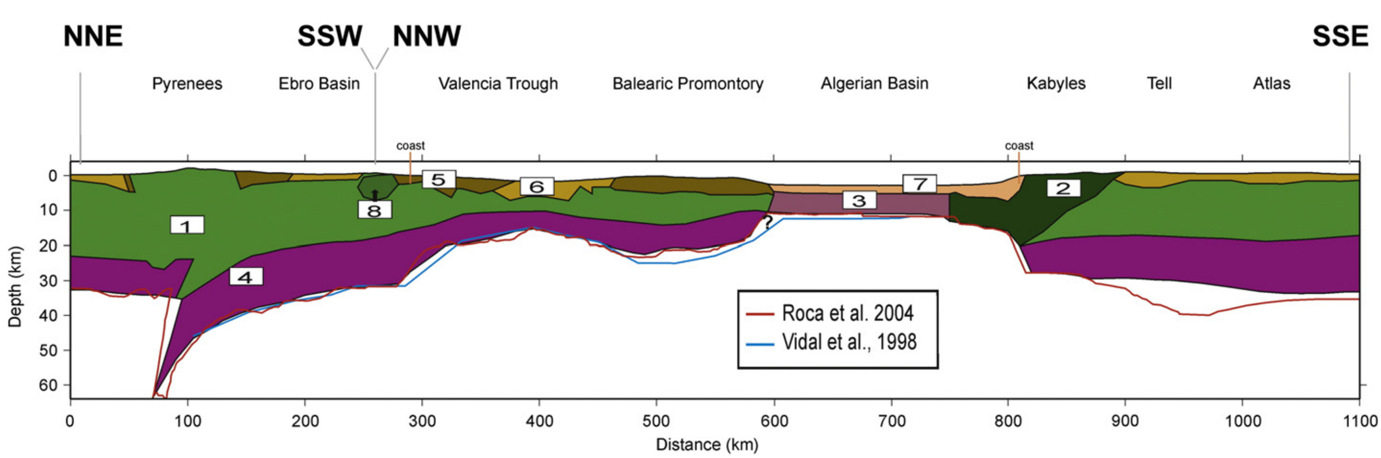

Fig. 3. Crustal structure corresponding to the best fitting model. Geometry of crustal bodies has been mainly taken from TRANSMED-II geotransect (Roca et al., 2004) based on ECORS—Central Pyrenees (ECORS Pyrenees Team, 1988), ESCI—Catalanides (Gallart et al., 1994), ESCI—Valencia (Vidal et al., 1998) and ALE-4 (industrial profile) seismic profiles. Blue and red lines refer to Moho depth proposed by Roca et al. (2004) and Vidal et al. (1998), respectively. Numbers denote crustal bodies summarized in Table 1.

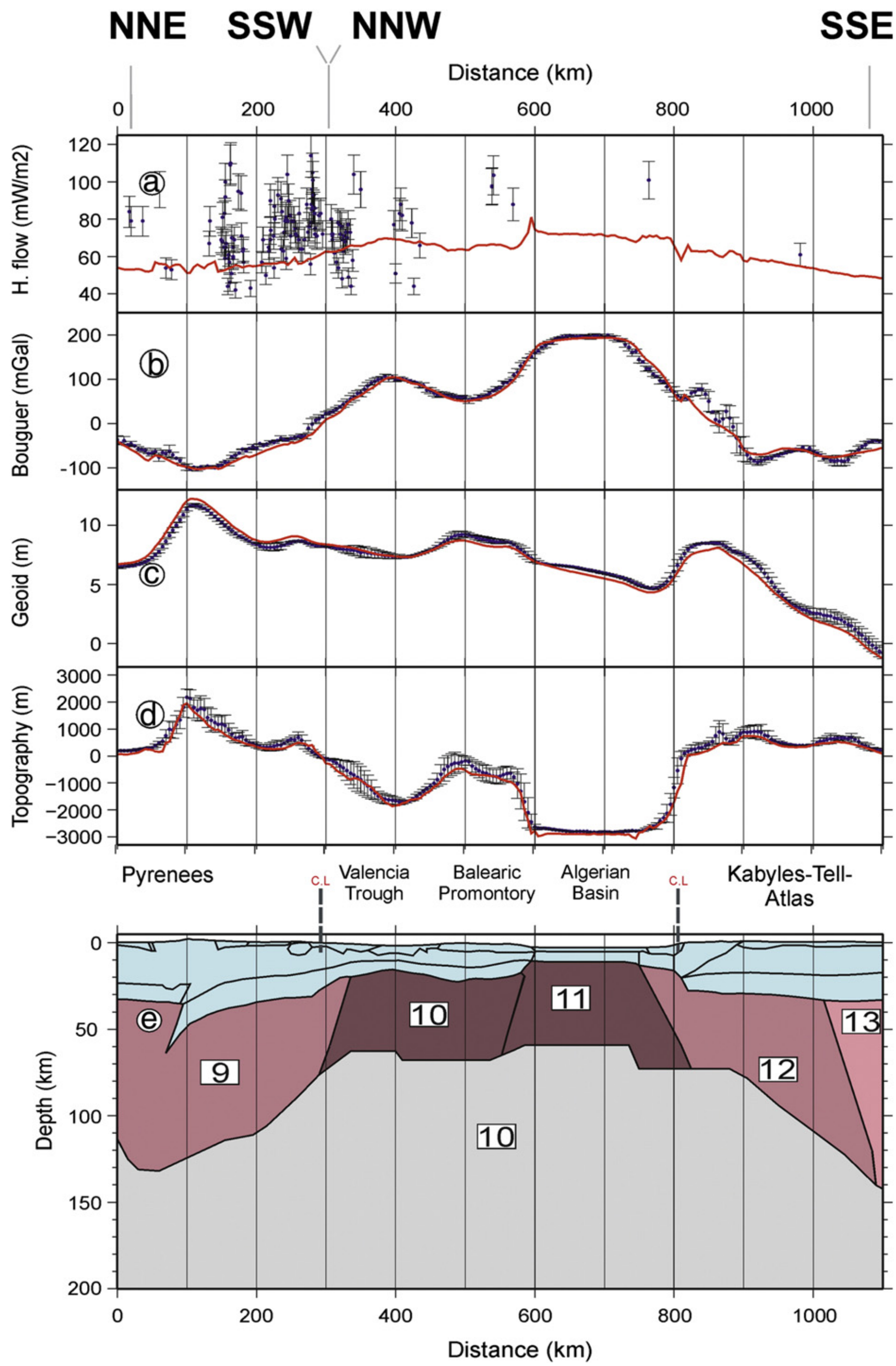

Fig. 4. Model results (red lines) and measured data with the standard deviation of data projected onto the profile within a strip of 25 km half-width (blue dots and vertical bars): (a) surface heat flow; (b) Bouguer anomaly; (c) geoid height; (d) elevation; (e) lithospheric structure. Crustal structure like in Fig. 3. Numbers in panel (e) denote mantle bodies summarized in Table 2. Dataset sources as in Fig. 2.

Table 1
Parameters used in the model for the different crustal bodies.

	Crust and sediments	Density (kg/m^3)	Heat production (μW/m^3)	Thermal conductivity (W/(K · m))
1	Upper crust	2780	1.0	3.10
2	Trans. upper crust	2840	1.0	3.10
3	Oceanic crust	2950	0.3	2.50
4	Lower crust	2900	0.3	2.50
5	Mesozoic sediments	2650	1.0	2.50
6	Cenozoic sediments	2550	1.0	2.40
7	Neogene sediments	2400	1.0	2.20
8	Tardi-hercynian plutons	2650	1.2	2.50

Table 2
Bulk mantle compositions used in the model.

	Mantle composition	SiO_2	Al_2O_3	FeO	MgO	CaO	Na_2O
9	Pr_6 (Lherz Av.)	45.4	3.7	8.3	39.9	3.2	0.26
10	Pm_1 (primitive uppermantle)	45	4.5	8.1	37.8	3.6	0.36
11	Pm_2 (primitive uppermantle)	45.2	4	7.8	38.3	3.5	0.33
12	Tc_1 (Av. Tecton)	44.5	3.5	8.0	39.8	3.1	0.24
13	TILE (tecton incipient)	44.97	2.33	8.32	40.18	2.52	0.18

resulting mantle corresponds to a primitive upper mantle (PUM, Pm_2) as defined by Jagoutz et al. (1979) which is in agreement with the continental highly intruded nature of the lithosphere, whereas the oceanic-type Algerian Basin is characterized by a more enriched PUM-type (Pm_1, McDonough and Sun, 1995). In the Alpine domain of North Africa, which includes the continental margin and the Kabyles–Tell–Atlas region, the obtained mantle corresponds to an average Phanerozoic-Tecton-type garnet-rich composition (Tc_1, Griffin et al., 2009), which differs noticeably from that obtained farther to the South corresponding to a more depleted 'tecton incipient or little extension' TILE composition, as already suggested by Griffin et al. (1999).

As observed in Fig. 4, calculated gravity, geoid and elevation match the observed regional trends. Major differences in Bouguer anomaly, up to 30 mGal, are observed locally in the Kabyles mountains probably related to local 3D crustal features not considered in our model. This misfit is also reflected in the calculated elevation reaching differences of < 500 m. Heat flow data is not so well constrained owing to its scarcity and associated uncertainty, particularly at the SE-half of the profile. Calculated values range from 55 to 60 mW m^{-2} in the Pyrenean domain increasingly steadily to 70–75 mW m^{-2} in the Valencia Trough basin and 75–80 mW m^{-2} in the Algerian basin. Towards the SE, the calculated heat flow decreases to minimum values of 50 mW m^{-2} at the south-easternmost tip of the profile. Certainly, the calculated surface heat flow is consistently lower (about 15%) than measured values along the whole profile. The main reason for this discrepancy is related to the calculated mantle thermal conductivities which have been computed using Hofmeister's P–T dependent approach (Hofmeister, 1999). Underestimation of thermal conductivity will affect essentially the calculated surface heat flow but will have minor effects on the calculated temperatures within the lithosphere and therefore on the mineral assemblages and resulting densities.

4.1. Crustal and lithosphere mantle structure

The resulting crustal structure (Figs. 3 and 4) shows minor differences with TRANSMED-II transect from the Pyrenees to the North-Africa margin. However, beneath the Kabyles–Tell–Atlas region, the modeled crust is up to 10 km thinner. In the Balearic Promontory, our results coincide with TRANSMED-II although the crust is slightly thinner with respect to Vidal et al. (1998).

Fig. 4 shows that the LAB depth varies along the model profile reaching depths of about 130 km beneath the Pyrenean chain, about 65 km and 70 in the Valencia Trough Basin and Balearic Promontory, respectively, shallowing to as much as 60 km in the Algerian Basin. A sharp thickening is observed in the transition from the basin to the continental margin of North Africa, from where the LAB progressively deepens to reach maximum depths of 140 km at the SE tip of the profile.

The resulting geometry of the LAB differs substantially from those obtained with previous models (Fig. 5). In the Pyrenean domain major discrepancies are observed with the results of a magneto-telluric study by Campanyà et al. (2012) where the LAB depth varies from 90 km beneath the Iberian Plate to 130 km in the Eurasian Plate. There are also differences with studies that have used similar integrated approaches. We obtain a similar lithospheric thickness to that proposed by Zeyen and Fernandez (1994) and a lower thickness than Roca et al. (2004) although our maximum thickness is slightly displaced 50 km to the North relative to these studies. Major discrepancies are observed in the style of thinning from the South Pyrenean Thrust to the continental shelf of the Valencia Trough Basin. Our results show a steady thinning of the lithosphere whereas models by Zeyen and Fernandez (1994) and Roca et al. (2004) suggest a step-like thinning resulting in differences of 15 km in the LAB depth over this region.

Underneath the Neogene Mediterranean basins the calculated LAB depth is very similar to that proposed by Ayala et al. (1996, 2003) and Zeyen and Fernandez (1994). However, our results show that the LAB beneath the Valencia Trough and Balearic Promontory is 10–15 km shallower and 10 km deeper beneath the Algerian Basin than that proposed by Roca et al. (2004). From the south Algerian Basin to the Kabyles–Tell–Atlas region the lithosphere thickens in a very different style compared to TRANSMED-II (Roca et al., 2004). These authors propose a sharp thickening from 55 to more than 160 km over a 200 km wide region, whereas our results show a more moderate step-like thickening from 60 to 140 km. Maximum differences of the LAB

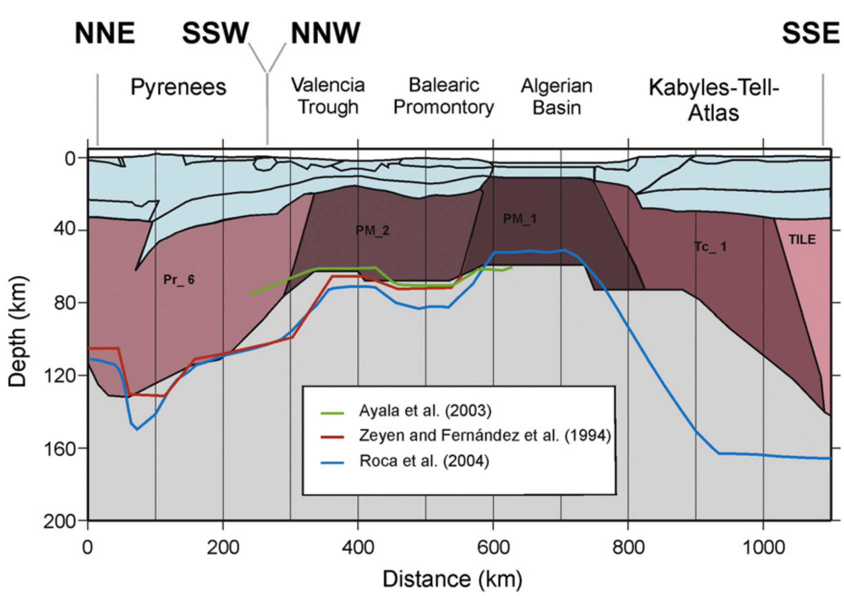

Fig. 5. Lithosphere structure of best fitting model and mantle domains with different chemical composition (see Table 2). Color lines denote LAB geometries proposed in previous studies.

depth between the two models reach as much as 70 km beneath the Tell Mountains. These discrepancies are mainly related to the poorly constrained crustal thickness considered in the TRANSMED-II transect (see below) and, to a lesser extent, to the different modeling approaches.

4.2. Mantle seismic velocities

One of the main advantages of the methodology used in this study is that LitMod allows calculating in a self-consistent way the elastic

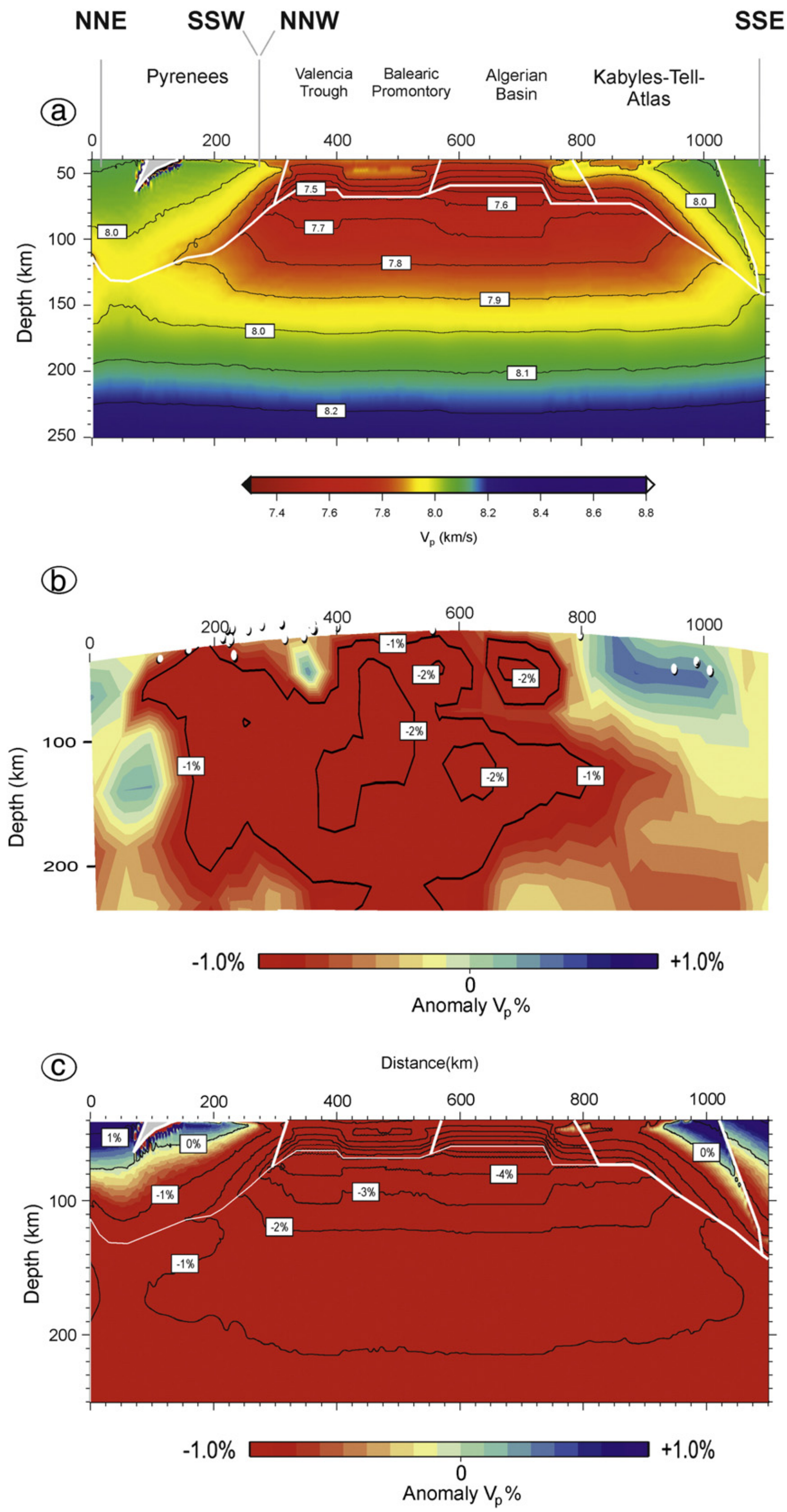

Fig. 6. a) Calculated P-wave seismic velocities in the upper mantle (calculations extend down to 410 km depth). White solid lines indicate mantle domains with different chemical composition. b) P-wave tomography model (Villaseñor et al., 2003) and c) synthetic P-wave tomography from our model. In both cases velocity anomalies are relative to the ak135 reference model. Contour lines every 1%.

parameters of the mantle and therefore the P and S-wave seismic velocities. Fig. 6a shows the calculated P-wave velocities in the mantle where low values at the LAB (7.5–7.6 km/s) are found underneath the Neogene Mediterranean basins and their continental margins. The low velocity values extend down to 150 km depth and are related to the relatively high T prevailing in this part of the sublithospheric mantle. Beneath the Pyrenean and Kabyles–Tell–Atlas domains P-wave velocities reach 8.0–8.1 km/s in the uppermost mantle decreasing slightly with depth until the LAB, defining a LVZ with variable thickness along the profile. Below 160 km depth, P-wave velocities increase with a constant gradient due to the prevailing effect of pressure.

Fig. 6b compares the global P-wave tomographic model of Villaseñor et al. (2003) with the synthetic tomographic model obtained from our calculated P-wave velocities expressed in percentage with respect to the ak135 reference model (Kennett et al., 1995). There is a coincidence in the low velocity zones predicted by both models though discrepancies are seen beneath the Pyrenees at depths higher than 100 km and below the Valencia Trough Basin. Also the amplitudes of the calculated low velocity anomalies are larger than those obtained in the tomographic model. The underestimation of the velocity anomalies by tomographic models based on ray theory is a well know result that is caused by the wavefront healing phenomenon (e.g. Hung et al., 2001). Therefore only the distribution and shape of the anomalies, not their amplitudes, can be meaningfully compared. In North Africa, the low resolution of the tomographic global model due to the poor coverage of available seismic stations does not allow for firm conclusions. Our results are also qualitatively consistent with the regional P-wave tomography model by Piromallo and Morelli (2003) that shows low velocities in the Western Mediterranean basins down to 400 km depth. Interestingly, these authors show relatively high velocities in the North Africa margin, particularly in eastern Algeria and Tunisia.

S-wave velocities show a similar pattern than P-wave (Fig. 7) with minimum values of <4.2 km/s in the sublithospheric mantle in the Western Mediterranean basins. Low S-wave velocities (<4.4 km/s) extend over the sublithospheric mantle down to 200 km depth from where they increase almost linearly with depth due to the effect of pressure. Within the lithospheric mantle, S-wave velocities increase from ~4.6 km/s in the uppermost mantle along the whole transect to 4.35 km/s in the LAB beneath the Pyrenees and the Kabyles–Tell–Atlas and <4.2 km/s beneath the Valencia Trough and the Algerian Basin.

A regional S-wave tomography model for Europe constrained by inversions of seismic waveforms (Legendre et al., 2012) shows pronounced negative anomalies ($\Delta Vs \sim -5\%$) in the Algerian Basin at 110 km depth, the amplitude of the anomaly decreasing with depth and vanishing below 200 km depth. According to this model, the Rif–Tell–Atlas region also shows negative Vs anomalies ($\Delta Vs \sim -3\%$) at 110 km depth. To compare our results with this tomography model we have plotted the resulting Vs values from Legendre et al. (2012) at different depth levels (80, 100, 150 and 200 km) according to the reference values used by these authors (Fig. 7). In general, our results fit well with the tomographic model although in the sublithospheric mantle our velocities are slightly higher beneath the Algeria Basin and lower beneath the Pyrenees and the Algeria margin. These small discrepancies are probably related to the thermal boundary condition used in our model that assumes a constant temperature at 410 km depth and therefore cannot account for deeper thermal anomalies.

An additional constraint on seismic mantle velocities comes from Pn velocity data. Fig. 8 compares the calculated P-wave velocities in the uppermost lithospheric mantle with Pn estimates from different seismic experiments. Calculated and observed values are in agreement in the Pyrenees and in the Iberian margin of the Valencia Trough. Discrepancies arise in the Neogene Mediterranean Basins amounting between 0.05 and 0.15 km/s with the exception of a local value where differences exceed 0.2 km/s. Possible explanations on these departures between observed and modeled data will be discussed in the next section.

4.3. Temperature and density distribution

Temperature distribution in the whole modeled domain is calculated under the assumption of steady-state thermal regime and displayed in Fig. 9 down to 250 km depth. Thermal parameters are summarized in Table 1. The temperature at the crust–mantle boundary ranges from a maximum of 850 °C beneath the Pyrenees (65 km depth) to a minimum of 250 °C beneath the oceanic-type crust of the Algerian basin where the Moho shallows to 12 km depth. In the Pyrenean domain average Moho temperatures are of 600–650 °C decreasing to 400–500 °C in the Valencia Trough and Balearic Promontory. In the North African region, temperatures range from 500 to 700 °C. Temperatures at the sublithospheric mantle vary from 1330 to 1400 °C in the thermal buffer

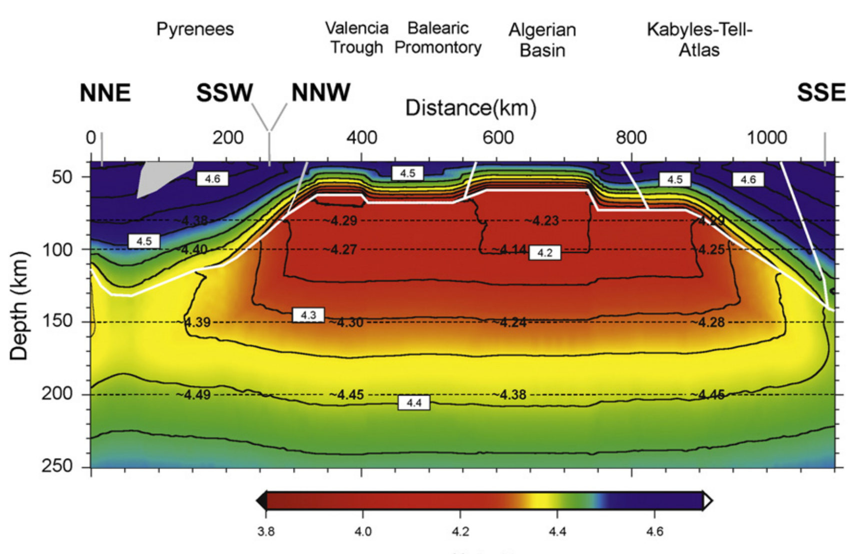

Fig. 7. Calculated S-wave seismic velocities in the upper mantle (calculations extend down to 410 km depth). White solid lines indicate mantle domains with different chemical composition. Contour lines every 0.05 km/s. Superimposed are the S-wave velocities inferred from the regional tomography model by Legendre et al. (2012) at different depth levels. S-values have been calculated according to the reference velocities of 4.38 km/s (at 80 and 110 km), 4.39 km/s (at 150 km) and 4.45 km/s (at 200 km) (see Legendre et al., 2012).

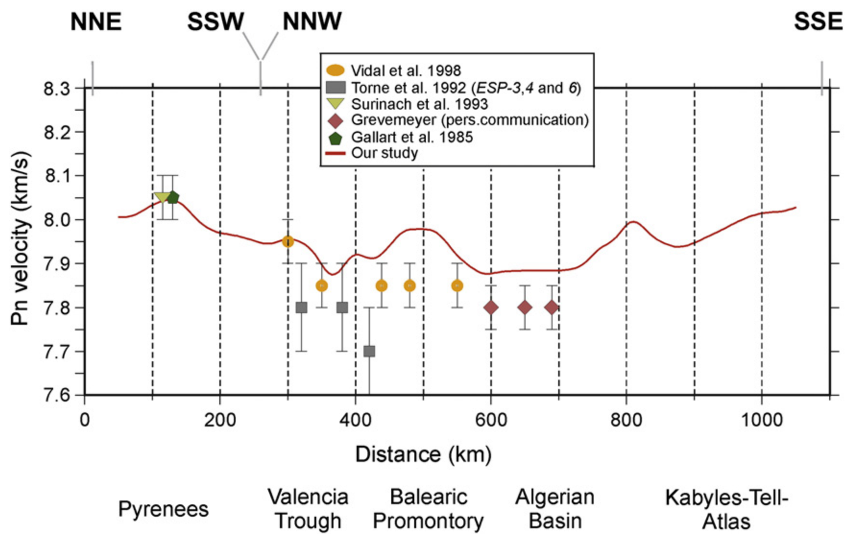

Fig. 8. Pn velocities along the modeled transect. Red line indicates calculated Pn values. Symbols with error bars denote Pn-values from seismic experiments (see legend).

increasing according to the adiabatic gradient from the base of the thermal buffer to the bottom of the model (410 km).

Densities in the crustal bodies are taken from literature and summarized in Table 1, whereas subcrustal densities are calculated according to mantle composition and thermodynamic formulation. Thereby Fig. 10 shows the mantle density distribution down to 250 km depth. In the Pyrenean domain and the Atlas region densities reach values around 3350 kg m^{-3} decreasing towards the Neogene extensional basins of the Mediterranean. In the Valencia Trough and Algerian basins the lithosphere mantle density decreases from ~3320 kg m^{-3} below the Moho to ~3260 kg m^{-3} at the LAB. Nevertheless, in the Algerian basin in the uppermost mantle the density decreases sharply to 3230 kg m^{-3} related to the shallow-depth plagioclase-spinel phase transition. In contrast, beneath the Balearic Promontory and the North-Africa continental margin, a maximum density of 3320 kg m^{-3} at ~50 km depth is calculated related to the spinel–garnet transition. In the North African continental margin there is a pronounced lateral density gradient with average densities increasing from 3300 kg m^{-3} in the continental shelf to 3350 kg m^{-3} in the Tell–Atlas region. From the LAB to the bottom of the model density increases steadily due to the predominant effect of pressure, e.g. at 250 km depth density reaches values of 3470 kg m^{-3}.

5. Discussion

Hereinafter we discuss the obtained results in terms of the three main goals of this work.

5.1. LAB topography

As previously mentioned, the crustal structure is well constrained from the numerous seismic experiments and integrated geophysical models carried out along the studied transect with the exception of

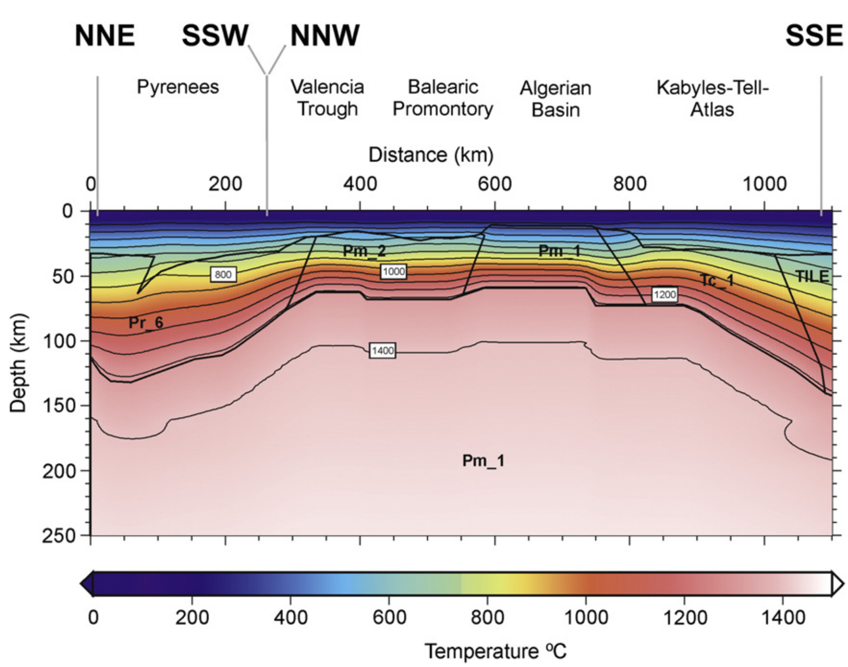

Fig. 9. Calculated temperature distribution along the modeled transect. Contour lines every 100 °C.

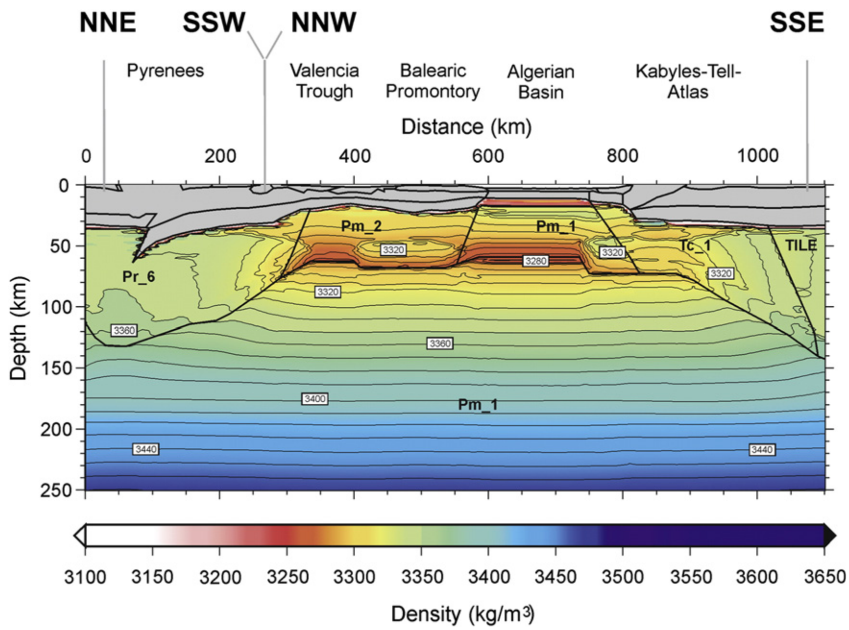

Fig. 10. Calculated mantle density distribution along the modeled transect. Contour lines every 10 kg m^{-3}. Sharp density increase in the uppermost mantle beneath the Algerian Basin is related to the Pg-Sp phase transition. Sharp density increase at ~40 km depth is related to Sp–Grt phase transition.

the onshore Algerian segment. However, the LAB topography relies solely on several models incorporating different datasets (e.g., Zeyen and Fernandez, 1994; Ayala et al., 1996; Ayala et al., 2003; Roca et al., 2004) and on mantle images from seismic tomography studies (e.g., Bijwaard and Spakman, 2000; Piromallo and Morelli, 2003; Villaseñor et al., 2003; Spakman and Wortel, 2004; Legendre et al., 2012). Since the obtained results have been already compared qualitatively to tomography models we will focus on the comparison with results obtained from previous integrated models.

Fig. 5 shows a comparison of our results with those obtained by Zeyen and Fernandez (1994), Ayala et al. (2003) and Roca et al. (2004). Below the Pyrenees, the differences observed are of 10–20 km with a displacement to the north of the maximum thickness probably related to differences in the crustal structure just beneath the axial zone of the Pyrenees. Underneath the Ebro foreland basin, the Catalan Coastal Ranges and the Iberian margin the LAB resulting from our model is consistently 20 km shallower than previously imaged by Zeyen and Fernandez (1994) and Roca et al. (2004) being in closer agreement with Ayala et al. (2003). Considering that the crustal structure is essentially the same as taken in previous models, the differences of the modeled LAB depth are related to the petrophysical approach we have adopted, which results in a different mantle density distribution. As mentioned, previous LAB studies by Zeyen and Fernandez (1994) and Roca et al. (2004) are based on a thermal approach in which the lithospheric mantle density is only temperature dependent and therefore, density decreases roughly linearly with depth through the thermal expansion coefficient. At difference, our modeling approach shows that in this segment of the transect (Ebro Basin–Catalan Coastal Ranges–Iberian margin) the lithosphere mantle density is nearly constant with depth and decreases laterally towards the Valencia Trough basin with a lateral gradient of 0.25 kg m^{-3} km^{-1} (Fig. 10).

The Algerian margin shows a similar lateral density gradient with increasing densities towards the Kabylies–Tell–Atlas region where a significantly thinner lithospheric mantle and a LAB depth up to 80 km shallower than imaged by Roca et al. (2004) are proposed. This significant discrepancy is attributed to two facts: a) the already mentioned differences in the depth-density distribution between the thermal and petrophysical approaches and b) the differences obtained in the crustal thickness which amount more than 10 km, from ca. 900 to 1000 km distance of the model transect (Fig. 3). The scarcity of deep seismic data in the region results in the lack of constraints on Moho depth, as a result our best fitting model shows a crust that is 10 km thinner than that proposed by Roca et al. (2004). As already mentioned by these authors, the onshore Algerian portion (Kabylies–Tell–Atlas) is fairly well constrained in its shallow part but poorly constrained at deep crustal levels, where no deep seismic data are available. Thus, the boundary between the upper and lower crust and the Moho geometry had to be drawn solely according to the results of previous gravity models (Mickus and Jallouli, 1999).

In the Mediterranean segment of the profile the results obtained in the Valencia Trough, Balearic Promontory and Algerian Basin, fairly coincide with those obtained by Zeyen and Fernandez (1994) and Ayala et al. (2003) but differ slightly when compared with Roca et al. (2004). Discrepancies with results from these authors are of the order of 10 km attaining maximum values of 15 km in the Balearic Promontory (Fig. 5). The observed relative lithospheric thickening and thinning are partly attributed to the differences of the density distribution within the lithospheric mantle related to chemical composition and the typical spinel–garnet phase transition occurring beneath the Balearic Promontory (Fig. 10) (see Afonso et al., 2008 for further details).

5.2. Changes in mantle composition

As pointed out by many authors, the structure of the Earth's upper mantle in continental areas is highly heterogeneous and much of the heterogeneity is associated with the thermal and compositional structure of the lithosphere. The composition of the sub-continental lithospheric mantle (SCLM) may range from refractory dunites and harzburgites to lherzolites depending on the degree of depletion in basaltic components through partial melting processes. These compositional heterogeneities may in turn translate in significant density differences at given *P*–T conditions related to compressibility, thermal expansion and phase transitions. Consequently, changes in mantle composition may affect modeling geophysical observables such as gravity, geoid, elevation, etc., since they are differentially sensitive to shallow and deep lateral density variations.

The *LitMod* approach characterizes chemically the lithospheric mantle to calculate density, temperature distribution and seismic wave velocities; therefore we have gathered all relevant information on mantle composition derived from geochemical analyses of outcrops

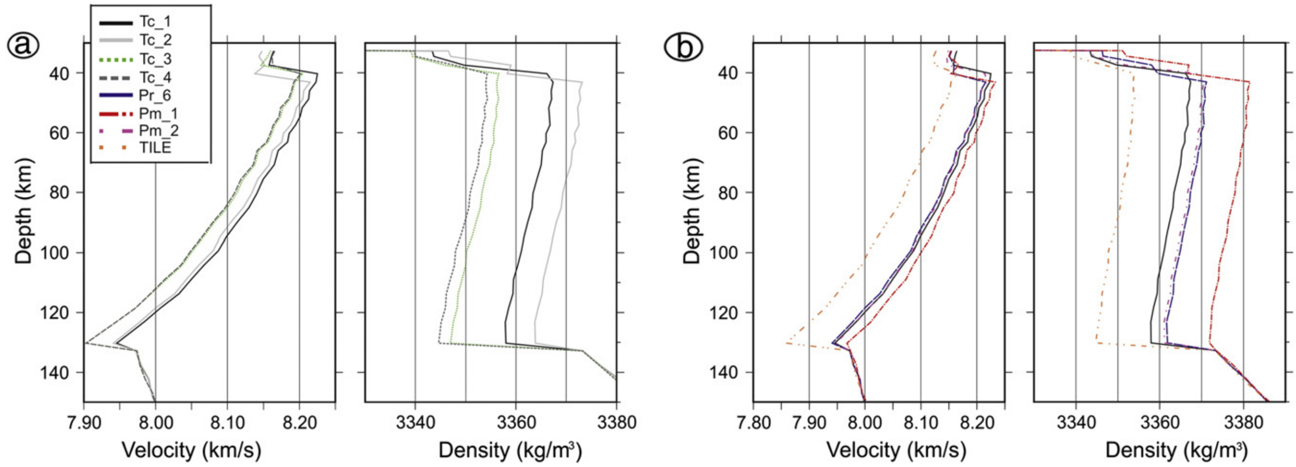

Fig. 11. a) Depth variation of P-wave velocities (left panel) and densities (right panel) calculated for different average-Tecton mantle compositions according to Griffin et al. (2009) for a 1-D lithosphere structure consisting of 32 km thick crust and 130 km thick lithosphere. b) Same as A for the mantle chemical compositions used in our modeled transect (see Table 2).

and/or global scale xenolith and tectonothermal age data (Table 2). Since some uncertainties have arisen in the composition of the SCLM of the North African margin due to the lack of xenolith information, we have tested four common Tecton bulk compositions (Tc_1 to Tc_4, Griffin et al., 2009) in accordance with the average tectonic age of the crustal units in the region. All four lithospheric mantle compositions are moderately depleted when compared to PUM composition. Fig. 11a shows the calculated P-wave velocities and densities for the different mantle compositions considering a standard lithosphere with a 32-km thick crust and a LAB depth of 130 km. As seen in Fig. 11a, beneath the Sp–Gnt transition at 40–45 km depth, no major differences are detectable in terms of absolute Vp velocities (of the order of 0.03–0.035 km s^{-1}, between Tc_1 and Tc_4), whereas maximum differences in SCLM density are of the order of 20 kg m^{-3} (between Tc_2 and Tc_4). From the four compositional models tested only the Tc_1 composition is found to better match the medium-long wavelength part of the geophysical observables (see Fig. 4), although it should be recognized that Tc_4 and likely Tc_2 and Tc_3 could be made compatible with the geophysical observables by slightly modifying the crust and mantle lithosphere geometry.

Fig. 11b summarizes the compilation of absolute Vp and densities calculated for the five compositional mantle types considered in this study with the same lithospheric structure as used in Fig. 11a. As observed, maximum velocity variations are of the order 0.1 km s^{-1} between the PUM composition of McDonough and Sun (1995) (Pm_1) and the TILE composition of Griffin et al. (1999). No major differences are observed in absolute Vp seismic velocities between the Proton lherzolite average type (Pr_6), the Tecton garnet type (Tc_1) and the primitive upper mantle compositions (Pm_1 and Pm_2). Results show that differences in Vp amount as much as 0.02 km s^{-1} for the Pm_1 composition, which are not detectable since they fall within the range of resolution of the seismic observable. Density differences at given *P*-T conditions attain maximum values of 28 kg m^{-3} between TILE and Pm_1; 10 to 15 kg m^{-3} between TILE and Tc_1, Pr_6 and Pm_2; and between Pm_1 and Tc_1, Pr_6 and Pm_2. Differences between Tc_1, Pr_6 and Pm_2 are <5 kg m^{-3}, the latest being barely detectable. Although no significant differences are observed in the calculated geophysical fingerprint of the proposed compositional mantle types, these areas are characterized by different tectonic ages and histories, and therefore it is likely that the mantle has retained different compositional signatures. Our best fitting model is compatible with a bulk mantle composition corresponding to Pr_6 underneath the Pyrenees as recorded from xenolith samples. This mantle-type composition is characterized by a relatively high content on CaO and Al_2O_3 (3.2 and 3.7%, respectively) which may represent Phanerozoic reworking of Proterozoic to Archean crust (Griffin et al., 2009).

Widespread Neogene volcanism in the W-Mediterranean basins supports a refertilization of the former mantle and therefore it is in agreement with the PUM mantle type found in this study. In the Valencia Trough magmatism is characterized by two volcanic cycles which are clearly separated in time and by their petrological setting (Martí et al., 1992). The first volcanic cycle being of Chattian-early Burdigalian is characterized by calc-alkaline andesitic and pyroclastic rocks, while the second of Tortonian to Recent age is characterized by poorly differentiated alkali-basalts. The Pm_2 mantle composition used in the Valencia Trough and Balearic Promontory is similar to that used by Fullea et al. (2010) in the western part of the Atlas region where young alkaline magmatism is also present. Seismic data show that the Algerian Basin is floored by oceanic-type crust formed during Miocene times (Booth-Rea et al., 2007) and therefore, a more enriched composition relative to Pm_2 is justified. The Pm_1 mantle-type was also selected by Fullea et al. (2010) as representative for the Alboran and Algerian basins.

In the North African margin our results are also in agreement with those obtained by Fullea et al. (2010) who concluded that a Tc_1 mantle composition produces the best regional fitting model and that this mantle type could be taken as a representative average for the whole SCLM in the Atlantic–Mediterranean transition zone. In the Sahara region we have taken a mean TILE composition to account for the transition to the West African Mobile Zone, which is characterized by largely reworked terranes including Archean/Proterozoic/Phanerozoic signatures (Begg et al., 2009).

Since LitMod2D code works under a forward scheme, it is not easy to precisely assess the role the different variables have on the resulting model. Identifying mantle density with bulk composition and seismic velocities is a difficult problem due to the lack of uniqueness. Recent works by Afonso et al. (2013a, 2013b) present a complete analysis of the trade-off between temperature and compositional effects on wave velocities, the non-uniqueness of the compositional space and the dissimilar sensitivities of physical parameters to temperature and composition. In these works, the authors conclude that a wide range of compositions can equally explain multiple geophysical data. As a consequence, deep temperature anomalies ≤150 °C and compositional anomalies ΔMg# < 3 are not simultaneously resolvable, being the bulk Al_2O_3 content a better compositional indicator than Mg#.

5.3. Low uppermost mantle Pn velocities

Anomalous low Pn velocities (Fig. 8) between 7.7 and 7.9 km s^{-1} have been reported by Torne et al. (1992), Vidal et al. (1998) and Grevemeyer (pers. comm.) underneath the Valencia Trough, the Balearic Promontory and the Algerian Basin coinciding with areas of

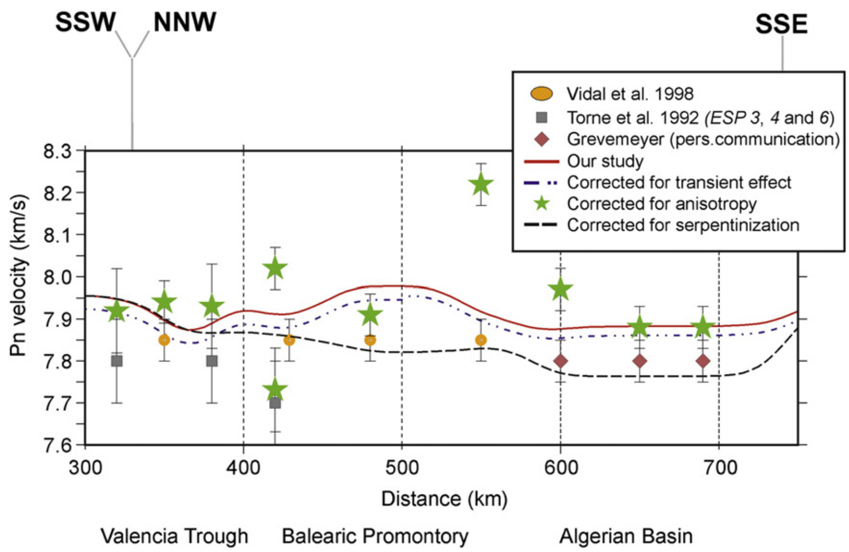

Fig. 12. Pn velocities along the W-Mediterranean segment of the modeled transect. Circles with error bars denote Pn values from seismic experiments (see Fig. 8 for data sources). Red solid line denotes calculated values from our model. Stars with error bars denote Pn values from seismic experiments corrected for anisotropy effects. Black solid line denotes calculated values corrected for thermal transient effects. Stippled black line denotes calculated values incorporating serpentinization. See text for details.

attenuated continental crust and oceanic crust. As observed in Fig. 12 velocities calculated from this study vary from 7.9 km/s underneath the Valencia Trough area increasing to almost 8.0 km/s below the Balearic Promontory while along the Algerian basin velocities decrease again to 7.9 km/s. These values are consistently higher than those obtained by seismic experiments, even considering the uncertainties commonly associated with seismic experiments (± 0.1 km/s).

Thereby, the calculated *P*–T conditions in the W-Mediterranean basins together with composition changes in the lithospheric mantle do not suffice to explain the measured Pn velocities. Several processes may cause low velocities in the uppermost mantle that are not included in our modeling approach. Among these, we have considered the presence of small amounts of hydrous phase in the uppermost mantle, anisotropy, and transient thermal effects related to the opening of the Western Mediterranean. The effects of these processes on the calculated Pn velocities are summarized in Fig. 12.

The presence of a hydrated uppermost mantle or serpentinization cannot be ruled out in view of the lithosphere thinning particularly beneath the Algerian Basin. Therefore we have assumed that a variable thick hydrated layer in which we have increased the water content to as much as 1% characterizes the uppermost mantle in the region. Fig. 12 shows the influence on the velocities of a hydrated layer that increases its thickness from 2 km underneath the Valencia Trough slightly thickening towards the Algerian Basin to as much as 4 km, and with a variable water content varying from 1% in the Valencia Trough area to 0.3% in the Algerian Basin. As observed, the presence of a hydrated uppermost mantle (dashed line in Fig. 12) allows fitting the calculated Pn velocities with those obtained from seismic experiments with maximum differences of the order 0.025 km/s.

Anisotropy is also a possible cause of mismatch between calculated and observed seismic velocities particularly when the fast polarity direction is perpendicular to the model transect. According to Díaz et al. (2013), anisotropic effects account for velocity variations ranging from minimum values of less than 0.075 km/s in the Algerian Basin to 0.3 km/s in the Balearic Promontory with the fast axis showing a predominantly E–W orientation in the Valencia Trough region switching to a NNE–SSW orientation in the Algerian Basin (see Fig. 9 of Díaz et al., 2013). Keeping in mind these considerations, the corrected velocities obtained from seismic experiments lay well within the calculated average values with the exception of the SE margin of the Valencia Trough and Balearic Promontory in which differences may reach locally more than 0.3 km/s.

Our numerical approach assumes thermal steady-state and therefore tends to underestimate the temperature prevailing at shallow levels of the lithospheric mantle and overestimate at deeper lithospheric levels in order to maintain the same buoyancy to that obtained from a linear steady-state geotherm. The temperature departures from steady-state geotherms can be easily calculated by considering instantaneous lithospheric thinning with a given beta-factor and occurring at a prescribed time according to McKenzie (1978). Maximum transient thermal effects are expected in the Algerian Basin where we have considered an extension factor of $\beta = 5$ to simulate generation of oceanic lithosphere and $t = 17$ Ma, resulting in a temperature difference of $\Delta T \approx 80$ K. This ΔT translates to a $\Delta Vp = -0.04$ km/s when a typical temperature derivative of $\partial Vp/\partial T = -0.5 \times 10^{-4}$ km s^{-1} K^{-1} for garnet peridotite is applied (Afonso et al., 2010). Fig. 12 shows that the thermal transient effect on Pn velocities is too small to account for misfits between measured and calculated P-wave velocities in the uppermost mantle.

As summary, the thermal and petrophysical characterization of the lithospheric mantle in NE-Iberia and western Mediterranean obeys to a complex plate reorganization since Jurassic times and probably earlier (Fig. 13). Our results are compatible with a predominantly typical Phanerozoic composition as indicated by Griffin et al. (2009) on the basis of global studies. Minor lateral variations in the continental domains are explained in terms of tardi-Hercynian plutonism in the Pyrenees which occurred at about 300–280 Ma and the transition towards a more stable lithosphere in the Sahara craton. Major chemical changes are related to the slab roll-back of the Ligurian-Tethyan ocean and the opening of the western Mediterranean basins occurred during the Neogene. The Valencia Trough basin underwent a prominent crust and lithospheric mantle thinning with asthenospheric upwelling and large alkaline magmatic intrusions and volcanism with a chemical refertilization of the lithospheric mantle. In the Algerian basin, backarc extension produced the generation of new oceanic crust and a more fertile mantle than in the Valencia Trough. Extension related to slab roll-back would be also responsible for partial serpentinization of the uppermost mantle and the measured low Pn velocities in the Valencia Trough and the Algerian Basin.

6. Conclusions

We have presented a new lithospheric modeling along the TRANSMED-II geotransect crossing the NE-Iberian Peninsula, the Western Mediterranean basins and the Algerian margin, ending at the

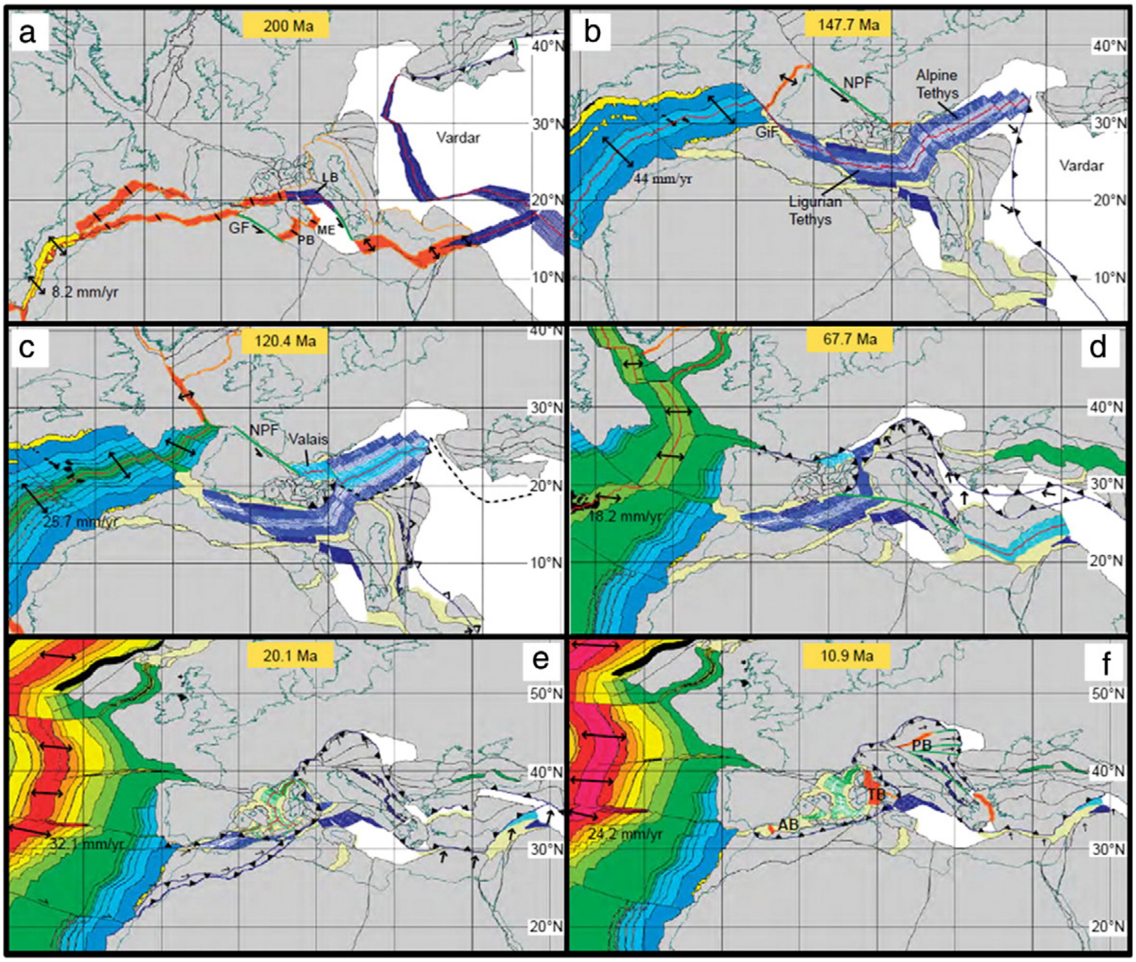

Fig. 13. Plate tectonic maps showing the evolution of Africa, Iberia and Europe from early Jurassic to late Miocene according to Schettino and Turco (2010). Main tectonic episodes correspond to: a) Initiation of rifting in the Central Atlantic ocean and the Africa–Iberia–Eurasia plate boundary; b) Opening of the Alpine and Ligurian-Tethys oceanic domains and initiation of rifting in the North-Atlantic; c) Opening of the North-Atlantic and Valais ocean and eastern escape of Iberia and early Alpine subduction; d) Pyrenean orogeny with successive phases of initiation of shortening, Paleocene standstill and restart of Pyrenean and Alpine orogeny; e) Atlas orogeny and subduction of the Ligurian-Tethys oceanic domain; and f) Trench retreat in the Alboran–Tyrrhenian–Pannonian domains.
Adapted from Schettino and Turco (2010).

Tell–Atlas region and based on the LitMod-2D approach. The approach integrates geopotential, lithostatic and thermal equations and, unlike previous models carried out in the region, incorporates petrophysical and geochemical data of the mantle down to 410 km depth. The main contribution of this model is the calculation of temperatures, densities, and seismic velocities (Vp and Vs) in the upper mantle as a function of prevailing *P*–T conditions and chemical compositions and therefore mineral assemblages and phase transitions. Results can be compared with gravity, geoid, elevation, surface heat flow and also with xenolith and seismic data and tomography models.

The main conclusions arising from the presented study are:

- The resulting lithospheric structure shows large variations in crust and lithospheric mantle thickness. At crustal level, our results confirm previous findings in that relative maximum crustal thickness is attained in the Pyrenees (up to 60 km), the Balearic Promontory (25 km) and the Kabyles–Tell–Atlas mountains (30–35 km), whereas relative minimum values are found in the Valencia Trough (16 km) and the Algerian Basin (10 km). At mantle lithosphere level, we observe that the LAB depth varies from 130 km beneath the Pyrenees to 65 km in the Valencia Trough, 70 km in the Balearic Promontory and 60 km in the Algerian Basin. A sharp thickening is obtained towards the N-African margin, the LAB deepening to 140 km beneath the Tell–Atlas Mountains.
- Major differences with respect to previous works are found beneath the Tell Mountains where our modeled crust is 10 km thinner (30 km Moho depth) than proposed in the TRANSMED-II geotransect. The LAB geometry shows also conspicuous differences with some of the previous works, particularly beneath the Ebro Basin and Catalan Coastal Ranges where our LAB is up to 20 km shallower and beneath the Algerian margin and the Kabyles–Tell–Atlas region where our lithosphere is up to 80 km thinner, with maximum thicknesses located underneath the Saharan platform.
- We have distinguished five mantle domains according to its chemical composition inferred from xenolith data and/or tectonothermal age. In the emerged continental mainland we used a predominant Phanerozoic average mantle composition though in NE-Iberia we used a lherzolitic Proterozoic mantle. In the W-Mediterranean basins we used a PUM composition distinguishing between the highly extended and intruded Valencia Trough and Balearic Promontory and the more enriched lithospheric mantle of the oceanic Algerian Basin and the underlying asthenosphere.
- Though the mantle compositions cannot be resolved univocally, the chosen compositions are compatible with the global geochemical xenolith data and the tectonothermal age of the different domains included in the modeled transect. Indeed, the different mantle compositions result in moderate differences in relevant observables as P-wave seismic velocities and densities. However, the density distribution

within the lithospheric mantle, which incorporates pressure, temperature and phase transition effects, differs substantially from that expected from a pure thermal approach and is responsible for the major differences in the obtained LAB geometry.

- The low Pn velocities recorded from seismic experiments in the W-Mediterranean basins can be explained by either moderate serpentinization in the first 3–4 km of the uppermost mantle, or seismic anisotropy. Transient thermal effects do not suffice to explain the measured Pn velocities. Evidently a combination of the three processes is also plausible.

Acknowledgments

The presented work has been supported by Topo-Iberia Consolider-Ingenio CSD2006-0004 and GASAM/TopoMed (CGL2008-03474-E/BTE/07-TOPO-EUROPE-FP-006) projects. AC benefitted from a JAE-PreCP grant from CSIC.

References

Afonso, J.C., Fernandez, M., Ranalli, G., Griffin, W.L., Connolly, J.A.D., 2008. Integrated geophysical–petrological modelling of the lithospheric–sublithospheric upper mantle: methodology and applications. Geochemistry, Geophysics, Geosystems 9, Q05008. http://dx.doi.org/10.1029/2007GC001834.

Afonso, J.C., Ranalli, G., Fernandez, M., Griffin, W.L., O'Reilly, S.Y., Faul, U., 2010. On the Vp/Vs–Mg# correlation in mantle peridotites: implications for the identification of thermal and compositional anomalies in the upper mantle. Earth and Planetary Science Letters 289, 606–618.

Afonso, J.C., Fullea, J., Griffin, W.L., Yang, Y., A. G., Jones, A.G., Connolly, J.A.D., O'Reilly, S.Y., 2013a. 3D multi-observable probabilistic inversion for the compositional and thermal structure of the lithosphere and upper mantle I: a priori information and geophysical observables. Journal of Geophysical Research Solid Earth 118, 2586–2617. http://dx.doi.org/10.1002/jgrb.5012423.

Afonso, J.C., Fullea, J., Yang, Y., Connolly, J.A.D., Jones, A.G., 2013b. 3D multi-observable probabilistic inversion for the compositional and thermal structure of the lithosphere and upper mantle II: general methodology and resolution analysis. Journal of Geophysical Research Solid Earth 118, 1650–1676. http://dx.doi.org/10.1002/jgrb.50123.

Argus, D.F., Gordon, R.G., Demets, C., Stein, S., 1989. Closure of the Africa–Eurasia–North America plate circuit and tectonics of the Gloria fault. Journal of Geophysical Research 94, 5585–5602.

Ayala, C., 2013. A new compilation of gravity data over the Iberian Peninsula and surrounding areas. Internal Report TopoIberia project (Consolider-Ingenio)IGME (20 pp.).

Ayala, C., Pous, J., Torné, M., 1996. The lithosphere–asthenosphere boundary of the Valencia trough (western Mediterranean) deduced from 2D geoid and gravity modeling. Geophysical Research Letters 22, 3131–3134.

Ayala, C., Torne, M., Pous, J., 2003. The lithosphere–asthenosphere boundary in the western Mediterranean from 3D joint gravity and geoid modelling: tectonic implications. Earth and Planetary Science Letters 209, 275–290.

Begg, G., Griffin, W.L., Natapov, L.M., O'Reilly, S.Y., Grand, S., O'Neill, C.J., Poudjom-Djomani, Y., Deen, T., Hronsky, J., Bowden, P., 2009. The lithospheric architecture of Africa: seismic tomography, mantle petrology and tectonic evolution. Geosphere 5, 23–50. http://dx.doi.org/10.1130/GES00179.1.

Bijwaard, H., Spakman, W., 2000. Non-linear global p-wave tomography by iterated linearized inversion. Geophysical Journal International 141, 71–82.

Booth-Rea, G., Ranero, C.R., Martínez-Martínez, J.M., Grevemeyer, I., 2007. Crustal types and Tertiary tectonic evolution of the Alborán Sea, western Mediterranean. Geochemistry, Geophysics, Geosystems 8, 1–25. http://dx.doi.org/10.1029/2007GC001639.

Campanyà, J., Ledo, J., Queralt, P., Marcuello, A., Liesa, M., Muñoz, J.A., 2012. New geoelectrical characterisation of a continental collision zone in the West-Central Pyrenees: constraints from long period and broad band magnetotellurics. Earth and Planetary Science Letters 333–334, 112–121.

Carminati, E., Wortel, M.J.R., Meijer, P.T., Sabadini, R., 1998. The two stage opening of the western–central Mediterranean basins: a forward modeling test to a new evolutionary model. Earth and Planetary Science Letters 160, 667–679.

Cavazza, W., Roure, F., Spakman, W., Stampfli, G.M., Ziegler, P.A. (Eds.), 2004. The TRANSMED Atlas — the Mediterranean Region from Crust to Mantle. Springer, Berlin Heidelberg. http://dx.doi.org/10.1007/978-3-642-18919-7.

Collier, J.S., Buhl, P., Torne, M., Watts, A.B., 1994. Moho and lower crustal reflectivity beneath a young rift basin — results from a 2-ship, wide-aperture seismic-reflection experiment in the Valencia Trough (western Mediterranean). Geophysical Journal International 118, 159–180.

Danobeitia, J.J., Arguedas, M., Gallart, F., Banda, E., Makris, J., 1992. Deep crustal configuration of the Valencia trough and its Iberian and Balearic borders from extensive refraction and wide-angle reflection profiling. Tectonophysics 203, 37–55.

DeMets, C., Gordon, R.G., Argus, D.F., Stein, S., 1994. Effect of recent revisions to the geomagnetic reversal time scale on estimate of current plate motions. Geophysical Research Letters 21, 2191–2194.

Deverchere, J., Yelles, K., Domzig, A., Mercier de Lepinay, B., Bouillin, J.P., Gaulier, R., Bracene, V., Calais, E., Savoye, B., Kherroubi, A., Le Roy, P., Pauc, H., Dan, G., 2005. Active thrust faulting offshore Boumerdes, Algeria, and its relation to the 2003 Mw 6.9 earthquake. Geophysical Research Letters 32. http://dx.doi.org/10.1029/2004GL021646.

Díaz, J., Gil, A., Gallart, J., 2013. Uppermost mantle seismic velocity and anisotropy in the Euro-Mediterranean region from Pn and Sn tomography. Geophysical Journal International. http://dx.doi.org/10.1093/gji/ggs016.

Doglioni, C., Gueguen, E., Sàbat, F., Fernandez, M., 1997. The Western Mediterranean extensional basins and the alpine orogen. Terra Nova 9 (3), 109–112.

Domzig, A., Le Roy, C., Yelles, K., Deverchere, J., Bouillin, J.-P., Bracene, R., Mercier de Lepinay, B., Le Roy, P., Calais, E., Kherroubi, A., Gaullier, V., Savoye, B., Pauc, H., 2006. Searching for the Africa–Eurasia Miocene boundary offshore western Algeria (MARADJA'03 cruise). Comptes Rendus Geoscience 338, 80–91.

Eaton, D.W., Darbyshire, F., Evans, R.L., Grütter, H., Jones, A.G., Yuan, X., 2009. The elusive lithosphere–asthenosphere boundary (LAB) beneath cratons. Lithos 109, 1–22.

ECORS Pyrenees team, 1988. The ECORS deep reflection seismic survey across the Pyrenees. Nature 311, 508–511.

Faccenna, C., Piromallo, C., Crespo-Blanc, A., Jolivet, L., Rossetti, F., 2004. History of subduction and back-arc extension in the central Mediterranean. Geophysic Journal International 145, 809–820.

Fernandez, M., Torne, M., Zeyen, H., 1990. Lithospheric thermal structure in NE Spain and North-Balearic basin. Journal of Geodynamics 12, 253–267.

Fernandez, M., Marzan, I., Correia, A., Ramalho, E., 1998. Heat flow, heat production, and lithospheric thermal regime in the Iberian Peninsula. Tectonophysics 291, 29–53. http://dx.doi.org/10.1016/S0040-1951(98)00029-8.

Fischer, K.M., Ford, H.A., Abt, D.L., Rychert, C.A., 2010. The lithosphere–asthenosphere boundary. Annual Review of Earth and Planetary Sciences 38, 551–575. http://dx.doi.org/10.1146/annurev-earth-040809-152438.

Foucher, J.E., Mauffret, A., Steckler, M., Brunet, M.E., Maillard, A., Rehanlt, J.E., Alonso, B., Desegaulx, E., Murillas, J., Ouillon, G., 1992. Heat flow in the Valencia trough: geodynamic implications. Tectonophysics 203, 77–97.

Fourcade, S., Allègre, C.J., 1981. Trace elements behavior in granite genesis: a case study. The calc-alkaline plutonic association from the Quérigut Complex (Pyrenees, France). Contributions to Mineralogy and Petrology 76, 177–195.

Frizon de Lamotte, D., Saint-Bezar, B., Bracène, R., Mercier, E., 2000. The two steps of the Atlas building and geodynamics of the western Mediterranean. Tectonics 19, 740–761.

Fullea, J., Fernandez, M., Zeyen, H., 2008. FA2BOUG—a FORTRAN 90 code to compute Bouguer gravity anomalies from gridded free air anomalies: application to the Atlantic–Mediterranean transition zone. Computers & Geosciences 34, 1665–1681.

Fullea, J., Fernandez, M., Afonso, J.C., Verges, J., Zeyen, H., 2010. The structure and evolution of the lithosphere–asthenosphere boundary beneath the Atlantic–Mediterranean Transition Region. Lithos 120 (1–2), 74–95. http://dx.doi.org/10.1016/j.lithos.2010.03.003.

Gallart, J., Vidal, N., Dañobeitia, J.J., the ESCI-Valencia Trough Working Group, 1994. Lateral variations in the deep crustal structure at the Iberian margin of the Valencia trough imaged from seismic reflection methods. Tectonophysics 232, 59–75.

Griffin, W.L., O'Reilly, S.Y., Ryan, C.G., 1999. The composition and origin of sub-continental lithospheric mantle. In: Fei, Y., Berkta, C.M., Mysen, B.O. (Eds.), Mantle Petrology: Field observations and High-pressure Experimentation: a Tribute to Francis R. (Joe) Boyd. Geochemical Society Special Publication, vol. 6, pp. 13–45.

Griffin, W.L., O'Reilly, S.Y., Afonso, J.C., Begg, G., 2009. The composition and evolution of lithospheric mantle: a reevaluation and its tectonic implications. Journal of Petrology. http://dx.doi.org/10.1093/petrology/egn033.

Gueguen, E., Doglioni, C., Fernandez, M., 1998. On the post-25 Ma geodynamic evolution of the Western Mediterranean. Tectonophysics 298, 259–269.

Gunnell, Y., Zeyen, H., Calvet, M., 2008. Geophysical evidence of a missing lithospheric root beneath the Eastern Pyrenees: consequences for post-orogenic uplift and associated geomorphic signatures. Earth and Planetary Science Letters 276, 302–313.

Handy, M.R., Schmid, S.M., Bousquet, R., Kissling, E., Bernoulli, D., 2010. Reconciling plate-tectonic reconstructions of Alpine Tethys with the geological–geophysical record of spreading and subduction in the Alps. Earth-Science Reviews 102, 121–158.

Hinz, K., 1972. Results of seismic refraction investigations (Project Anna) in Western Mediterranean, south and north of the island of Mallorca. Bulletin Centre De Recherches Pau-SNPA 6 (2), 405–426.

Hofmeister, A.M., 1999. Mantle values of thermal conductivity and the geotherm from phonon lifetimes. Science 283, 1699–1706.

Hung, S.-H., Dahlen, F.A., Nolet, G., 2001. Wavefront healing: a banana-doughnut perspective. Geophysical Journal International 146 (2), 289–312.

Jagoutz, E., Palme, H., Baddenhausen, H., Blum, K., Cendales, M., Dreibus, G., Spettel, B., Lorenz, V., Wanke, H., 1979. The abundance of major, minor and trace elements in the Earth's mantle as derived from primitive ultramafic nodules. Proc. Lunar and Planetary Science Conference 10th, pp. 2031–2205.

Kennett, B.L.N., Engdahl, E.R., Buland, R., 1995. Constraints on seismic velocities in the Earth from travel times. Geophysical Journal International 122, 108–124.

Lachenbruch, A.H., Morgan, P., 1990. Continental extension, magmatism and elevation: formal relations and rules of thumb. Tectonophysics 174, 39–62.

Le Roux, V., Bodinier, J.-L., Tommasi, A., Alard, O., Dautria, J.-M., Vauchez, A., Riches, A.J.V., 2007. The Lherz spinel lherzolite: refertilised rather than pristine mantle. Earth and Planetary Science Letters 259, 599–612.

Legendre, C.P., Meier, T., Lebedev, S., Friederich, W., Viereck-Götte, L., 2012. A shear wave velocity model of the European upper mantle from automated inversion of seismic shear and surface waveforms. Geophysical Journal International 191, 282–304. http://dx.doi.org/10.1111/j.1365-246X.2012.05613.x.

Lustrino, M., Duggen, S., Rosenberg, C.L., 2011. The central–western Mediterranean: anomalous igneous activity in an anomalous collisional tectonic setting. Earth-Science Reviews 104, 1–40.

Martí, J., Mitjavila, J., Roca, E., Aparicio, A., 1992. Cenozoic magmatism of the Valencia trough (western Mediterranean): relationships between structural evolution and volcanism. Tectonophysics 203, 145–165.
Marzán Blas, I., 2000. Régimen térmico en la Península Ibérica. Estructura litosférica a través del Macizo Ibérico y el Margen Sur-Portugués. Tesis Doctoral Universidad de Barcelona (192 pp.).
Mauffret, A., 2007. The Northwestern (Maghreb) boundary of the Nubia (Africa) Plate. Tectonophysics 429, 21–44.
McDonough, W.F., Sun, S., 1995. The composition of the Earth. Chemical Geology 120, 223–253.
McKenzie, D.P., 1978. Some remarks on the development of sedimentary basins. Earth and Planetary Science Letters 25–32.
Michard-Vitrac, A., Albarede, F., Dupuis, C., Taylor Jr., H.P., 1980. The genesis of Variscan (hercynian) plutonic rocks: inferences from Sr, Pb and O studies on the Maladeta igneous complex, Central Pyrenees, Spain. Contributions to Mineralogy and Petrology 72, 57–72.
Mickus, K., Jallouli, C., 1999. Crustal structure beneath the Tell and Atlas Mountains (Algeria and Tunisia) through the analysis of gravity data. Tectonophysics 314, 373–385.
Morgan, P., Ramberg, I.B., 1987. Physical changes in the lithosphere associated with thermal relaxation after rifting. Tectonophysics 143, 1–11.
Muñoz, J.A., 1992. Evolution of a continental collision belt: ECORS—Pyrenees crustal balanced section. In: McClay, K.R. (Ed.), Thrust Tectonics. Chapman and Hall, London, pp. 235–246.
Muñoz, J.A., 2002. The Pyrenees, in the geology of Spain. In: Gibbons, W., Moreno, T. (Eds.), Geological Society of London, pp. 370–385.
Muñoz, J.A., Martínez, A., Vergés, J., 1986. Thrust sequences in the eastern Spanish Pyrenees. Journal of Structural Geology 8 (3/4), 399–405.
Pascal, G., Torné, M., Buhl, P., Watts, A.B., Mauffret, A., 1992. Crustal and velocity structure of the València trough (western Mediterranean), Part II. Detailed interpretation of five Expanded Spread Profiles. Tectonophysics 203, 21–35.
Pavlis, N.K., Holmes, S.A., Kenyon, S.C., Factor, J.K., 2008. An Earth Gravitational Model to Degree 2160: EGM 2008, presented at Session G3: "GRACE Science Applications". EGU, Vienna.
Piromallo, C., Morelli, A., 2003. P wave tomography of the mantle under the Alpine–Mediterranean area. Journal of Geophysical Research 108 (B2), 2065. http://dx.doi.org/10.1029/2002JB001757.
Poudjom Djomani, Y.H., O'Reilly, S.Y., Griffin, W.L., Morgan, P., 2001. The density structure of subcontinental lithosphere through time. Earth and Planetary Science Letters 184, 605–621.
Pous, J., Ledo, J., Marcuello, A., Daignieres, M., 1995. Electrical resistivity model of the crust and upper mantle from a magnetotelluric survey through the central Pyrenees. Geophysical Journal International 121, 750–762.
Rimi, A., Fernandez, M., Manar, A., Matsushima, J., Okubo, Y., Morel, J.L., 2005. Geothermal anomalies and analysis of gravity, fracturing and magnetic features in Morocco. World Geothermal Congress Antalya, Turkey, vol. 2, pp. 4–290.
Roca, E., Sans, M., Cabrera, L., Marzo, M., 1999. Oligocene to Middle Miocene evolution of the Central Catalan margin (North-western Mediterranean). Tectonophysics 315, 209–229.
Roca, E., Frizon de Lamotte, D., Mauffret, A., Bracène, R., Vergés, J., Benaouali, N., Fernandez, M., Muñoz, J.A., Zeyen, H., 2004. TRANSMED transect II. In: Cavazza, W., Roure, F., Spakman, W., Stampfli, G.M., Ziegler, P. (Eds.), The TRANSMED Atlas—the Mediterranean Region from Crust to Mantle. Springer, Berlin Heidelberg.
Rosenbaum, G., Lister, G.S., 2002. Reconstruction of the evolution of the Alpine–Himalayan Orogen. Journal of the Virtual Explorer 8, 105–124.
Rosenbaum, G., Lister, G.S., 2004. Neogene and Quaternary rollback evolution of the Tyrrhenian Sea, the Apennines and the Sicilian Maghrebides. Tectonics 23, TC1013. http://dx.doi.org/10.1029/2003TC001518.
Sàbat, F., Muñoz, J.A., Santanach, P., 1988. Transversal and oblique structures at the Serres de Llevant thrust belt (Mallorca Island). Geologische Rundschau 77, 529–538.
Sàbat, F., Roca, E., Muñoz, J.A., Vergés, J., Santanach, P., Masana, E., Sans, M., Estévez, A., Santisteban, C., 1997. Role of extension and compression in the evolution of the eastern margin of Iberia: the ESCI-València trough seismic profile. Revista de la Sociedad Geológica de España 8, 431–448.
Sandwell, D.T., Smith, W.H.F., 1997. Marine gravity from Geosat and ERS 1 satellite altimetry. Journal of Geophysical Research 102, 10,039–10,054.
Schettino, A., Turco, E., 2010. Tectonic history of the western Tethys since the Late Triassic. Geological Society of America Bulletin 123, 89–105. http://dx.doi.org/10.1130/B30064.1.
Sibuet, J.-C., Srivastava, S.P., Spakman, W., 2004. Pyrenean orogeny and plate kinematics. Journal of Geophysical Research 109, B08104. http://dx.doi.org/10.1029/2003JB002514.
Spakman, W., Wortel, M.J.R., 2004. A tomographic view on western Mediterranean geodynamics. In: Cavazza, W., Roure, F., Spakman, W., Stampfli, G.M., Ziegler, P. (Eds.), The TRANSMED Atlas—the Mediterranean region from crust to mantle. Springer, Berlin Heidelberg, pp. 31–52.
Stampfli, G.M., Borel, G.D., 2002. A plate tectonic model for the Paleozoic and Mesozoic constrained by dynamic plate boundaries and restored synthetic oceanic isochrones. Earth and Planetary Science Letters 196, 17–33.
Stich, D., Ammon, C.J., Morales, J., 2003. Moment tensor solutions for small and moderate earthquakes in the Ibero–Maghreb region. Journal of Geophysical Research 108 (B3), 2148. http://dx.doi.org/10.1029/2002JB002057.
Thybo, H., Artemieva, I.M., 2013. Moho and magmatic underplating in continental lithosphere. Tectonophysics (in press).
Torné, M., De Cabissole, B., Bayer, R., Casas, A., Daignières, M., Rivero, A., 1989. Gravity constraints on the deep structure of the Pyrenean belt along the ECORS profile. Tectonophysics 165, 105–116.
Torne, M., Pascal, G., Buhl, P., Watts, A.B., Mauffret, A., 1992. Crustal structure of the Valencia Trough (Western Mediterranean). Part 1. A combined refraction/wide angle reflection and near-vertical reflection study. Tectonophysics 203, 1–20.
Torné, M., Banda, E., Fernàndez, M., 1996. The Valencia Trough: geological and geophysical constraints on basin formation models. In: Ziegler, P.A., Horvàth, F. (Eds.), Peri-Tethys Memoir 2: Structure and Prospects of Alpine Basins and Forelands. Mémoires Muséum National d'Histore Naturelle, 170, pp. 103–128.
Vergés, J., Fernàndez, M., 2012. Tethys–Atlantic interaction along the Iberia–Africa plate boundary: the Betic–Rif orogenic system. Tectonophysics 579, 144–172. http://dx.doi.org/10.1016/j.tecto.2012.08.032.
Vergés, J., García-Senz, J.M., 2001. Mesozoic evolution and cenozoic inversion of the Pyrenean Rift. In: Ziegler, P.A., Cavazza, W., Robertson, A.H.F., Crasquin-Soleau, S. (Eds.), Peri-Tethys Memoir 6: Pery-Tethyan Rift/Wrench Basins and Passive Margins. Mémoires Muséum National d'Histore Naturelle, 186, pp. 187–212.
Vergés, J., Sàbat, F., 1999. Constraints on the western Mediterranean kinematic evolution along a 1,000-km transect from Iberia to Africa. In: Durand, B., Jolivet, L., Horváth, F., Séranne, M. (Eds.), On the Mediterranean Basins: Tertiary Extension within Alpine orogen. Geological Society London Special Publications, 134, pp. 63–80.
Verges, J., Millan, H., Roca, E., Muñoz, J.A., Marzo, M., Cirés, J., den Bezemer, T., Zoetemeijer, S., Cloethingh, R., 1995. Eastern Pyrenees and related foreland basins: Pre-, syn- and post-collisional crustal-scale cross-sections. Marine and Petroleum Geology 12, 903–916.
Vergés, J., Fernàndez, M., Martínez, A., 2002. The Pyrenean orogen: pre-, syn-, and post-collisional evolution. Journal of the Virtual Explorer 8, 55–84.
Vidal, N., Gallart, J., Danobeitia, J.J., 1998. A deep seismic transect from the NE Iberian Peninsula to the Western Mediterranean. Journal of Geophysical Research 103, 12381–12396.
Vilà, M., Fernandez, M., Jiménez-Munt, I., 2010. Radiogenic heat production variability of some common lithological groups and its significance to lithospheric thermal modeling. Tectonophysics 490, 152–164.
Villaseñor, A., Spakman, W., Engdahl, E.R., 2003. Influence of regional travel times in global tomographic models. Geophysical Research Abstracts. EAE03-A-08614, EGS-AGU-EUG Joint Assembly, Nice, France, vol. 5.
Vissers, R.L.M., Meijer, P.Th., 2012. Mesozoic rotation of Iberia: subduction in the Pyrenees? Earth-Science Reviews 110, 93–110.
Wilson, M., Bianchini, G., 1999. Tertiary–Quaternary magmatism within the Mediterranean and surrounding regions. London Geological Society, Special Publication 156, 141–168.
Zeyen, H., Fernandez, M., 1994. Integrated lithospheric modelling combining thermal, gravity, and local isostasy analysis: application to the NE Spanish geotransect. Journal of Geophysical Research 99, 18089–18102.
Ziegler, P.A., Roure, F., 1996. Architecture and petroleum systems of the Alpine Orogen and associated basins. In: Ziegler, P.A., Hòrvath, F. (Eds.), Structure and Prospects of Alpine Basinsand Forelands, Peri-Tethys. Mémoires Muséum National d'Histore Naturelle, 170, pp. 15–45.